ACTA Mineralogica Petrographica

ACTA MINERALOGICA-PETROGRAPHICA, FIELD GUIDE SERIES, VOL. 13, PP. 1–32.

From maars to lava lakes: Ultramafic and granulite xenoliths associated with the alkaline basaltic volcanism of the Pannonian Basin

Edited by CSABA SZABÓ*

Lithosphere Fluid Research Lab, Eötvös L. University, Pázmány Péter sétány 1/C, Budapest, H-1117 Hungary; cszabo@elte.hu (*corresponding author)

Written by CSABA SZABÓ[1], ISTVÁN KOVÁCS[2], JÚLIA DÉGI[3], KLÁRA KÓTHAY[4], KÁLMÁN TÖRÖK[2], KÁROLY HIDAS[5], PÉTER KÓNYA[6] AND MÁRTA BERKESI[1]

[1] Lithosphere Fluid Research Lab, Eötvös L. University, Pázmány Péter sétány 1/C, Budapest, H-1117 Hungary; cszabo@elte.hu
[2] Eötvös Loránd Geophysical Institute of Hungary, Kolumbusz u. 17-23, Budapest, H-1145 Hungary
[3] Research Institute of Solid State Physics and Optics, Hungarian Academy of Sciences, Konkoly-Thege Miklós út 29-33, Budapest, H-1121 Hungary
[4] Department of Mineralogy, Eötvös L. University, Pázmány Péter sétány 1/C, Budapest, H-1117 Hungary
[5] Andalusian Institute of Earth Sciences, University of Granada, Facultad de Ciencias, Campus de Fuentenueva, 18071, Granada, Spain
[6] Geological Institute of Hungary, Stefánia út 14, Budapest, H-1143 Hungary

Table of contents

1. Geological introduction to the area visited

1.1 General introduction to the geology of the Carpathian-Pannonian Region (CPR)

The Carpathian-Pannonian region (CPR), which consists of a group of young extensional basins in the eastern neighbourhood of the Alpine orogen, is one of the geologically best studied areas in the world (*e.g.*, Fodor *et al.*, 1999; Csontos & Vörös, 2004; Szabó *et al.*, 2004; Horváth *et al.*, 2006). Its complex geology and geodynamic history has been recognized for a long time but, with some exceptions, has not been put in the wider geodynamic context. The fact that orogenic and extensional processes are relatively young, and that there is a massive body of knowledge on geology, geophysics, volcanism, crustal and mantle xenoliths and sediments provides us with a unique natural laboratory to test a range of possible models for the formation of extensional basins adjacent to orogens. New approach in the interpretation of Cenozoic volcanism (Kovács *et al.*, 2007), data on mantle xenoliths (Bali *et al.*, 2007; Falus *et al.*, 2007; Bali *et al.*, 2008a, 2008b; Szabó *et al.*, 2009), and seismic tomography (Grad *et al.*, 2006) raise challenges for the present geodynamical interpretation(s) and call for alternative explanations in future research.

1.1.1 The geodynamic framework and major tectonic units in the Carpathian-Pannonian region

The wider region comprises several mountain chains, *i.e.* the Eastern Alps, the Carpathian arc and the Dinarides, which surround the Intra-Carpathian Basin System, the internal part of which is commonly referred to as the Pannonian Basin. The Intra-Carpathian Basin System has a significantly extended continental crust, outcropping in several smaller internal mountains, and is filled by young sediments. Based on the Mesozoic tectonostratigraphy and structural analysis, the internal area is subdivided into two major units (Csontos, 1995; Csontos & Vörös, 2004; Haas *et al.*, 1995, 2000;

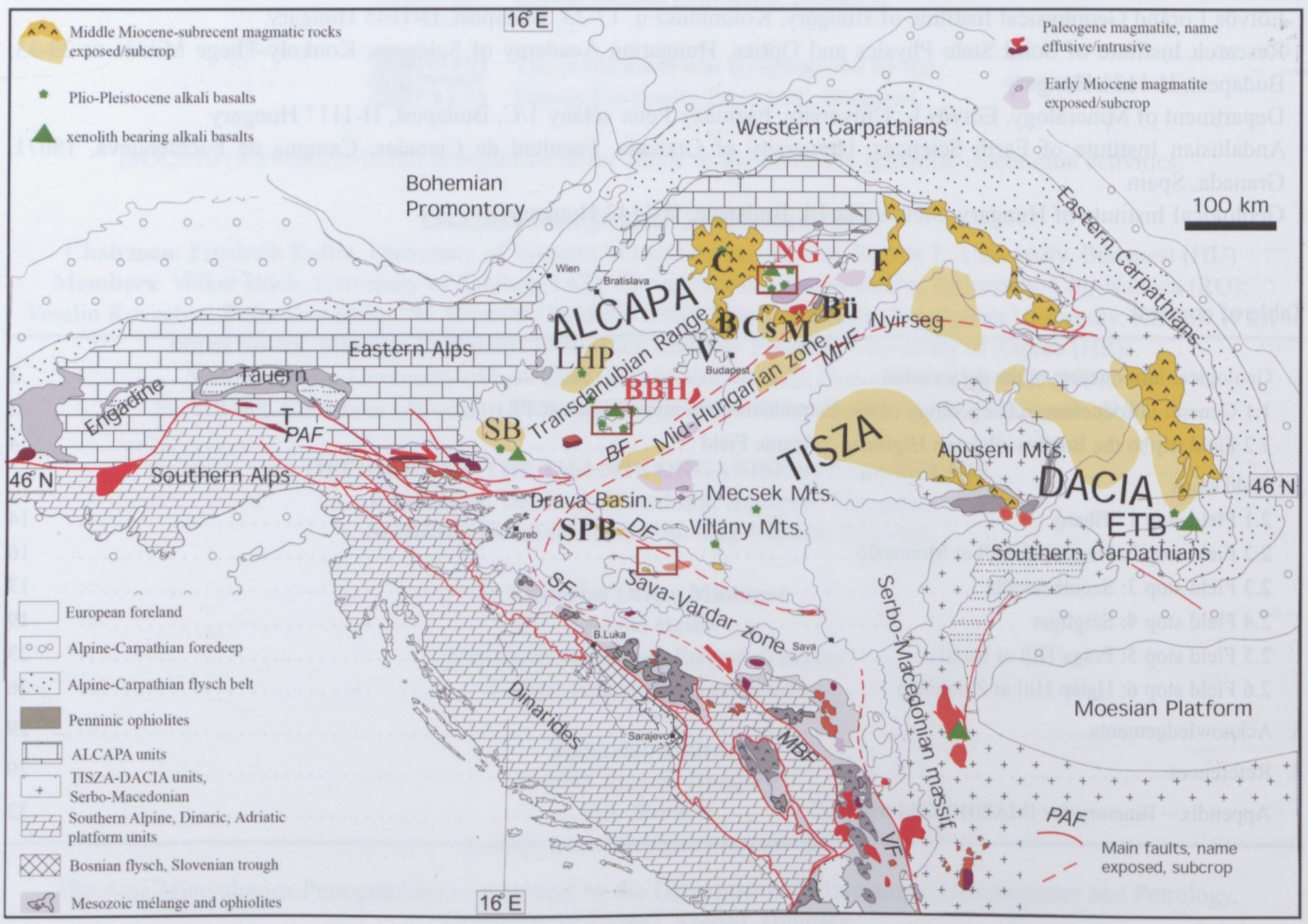

Fig. 1. Major tectonic units of the wider Carpathian-Pannonian region. The map is modified after Kovács *et al.* (2007). Plio-Pleistocene alkali basalts with mantle and lower crustal xenoliths are also highlighted (BBH – Bakony–Balaton Highland, LHP – Little Hungarian Plain volcanic field, NG – Nógrád–Gömör volcanic field, SB – Styrian basin, ETB – East Transylvanian basin). Some Paleogene–Early Miocene and Middle Miocene rocks are also indicated. The Bakony–Balaton Highland and Nógrád–Gömör are indicated by red letters.

Kovács *et al.*, 2000): ALCAPA (ALps-CArpathians-PAnnonian, *i.e.* northern Intra-Carpathian Basin System and Western Carpathians) and Tisza-Dacia (southern Intra-Carpathian Basin System; East and South Carpathians) (Fig. 1). Because of its distinct evolution during the Paleogene –Early Miocene, a further structural element can be distinguished. This is the Mid-Hungarian zone (Fig. 1), composed of the Bükk Mts. (N Hungary) and a narrow structural belt between Lake Balaton and the Mecsek Mts. (SW Hungary). It is composed of low- to high-pressure metamorphic Paleozoic–Mesozoic continental margin sediments, a mélange, and dispersed remains of a Jurassic ophiolite nappe (Wein, 1969; Haas *et al.*, 2000; Csontos & Vörös, 2004). The ALCAPA unit is defined as the unit bounded to the south by the Periadriatic and Balaton faults (Balla, 1984; Csontos, 1995; Fodor *et al.*, 1998, 1999). The Balaton fault separates ALCAPA from the Mid-Hungarian zone. The major fault separating the Mid-Hungarian unit from the Tisza-Dacia unit to the south is referred to as the Mid-Hungarian (or Zagreb-Zemplin) fault (Balla, 1984; Csontos & Nagymarosy, 1998; Haas *et al.*, 2000) (Fig. 1).

1.1.2 The geodynamic evolution of the Carpathian-Pannonian region

The study area was formed in three major steps during Tertiary (Csontos *et al.*, 1992; Csontos, 1995; Fodor *et al.*, 1999). The earliest tectonic phase took place in the Paleogene as a major right lateral shear event along the Periadriatic zone and the Balaton fault. This shear event was initiated in the Late Eocene (Fodor *et al.*, 1992); however, the main phase of shearing appears to have occurred during the Oligocene. As a consequence, ALCAPA was subjected to major right lateral displacement (Kázmér & Kovács, 1985) (Fig. 2). The next tectonic phase was dominated by opposite rotations of the ALCAPA and Tisza-Dacia microplates within the CPR (Márton, 1987; Csontos *et al.*, 1992). Based on paleomagnetic data, the two microplates were detached from their southern neighbour, the Dinarides, and were pushed or rotated into the Carpathian embayment during the Early Miocene (~20–18 Ma) (Fig. 2). The last major tectonic phase was the extension in the CPR. The extension may have happened in two distinct phases in the Middle (17–14 Ma) and Late Miocene (12–8 Ma). The first phase is often referred to as the 'active' phase characterized by active asthenospheric upwelling that caused equal thinning in the crust and lithospheric mantle of the entire CPR (Bada & Horváth, 2001; Huismans *et al.*, 2001). The second, 'passive', extensional episode that was due to the collapse of the asthenospheric dome only affected the central part of the CPR and resulted in more significant stretching of the lithospheric mantle (Bada & Horváth, 2001; Huismans *et al.*, 2001). This is also reflected in the lithospheric thickness as it is the smallest in the centre and increases towards the edges of the CPR (Horváth, 1993) (Fig. 3). This

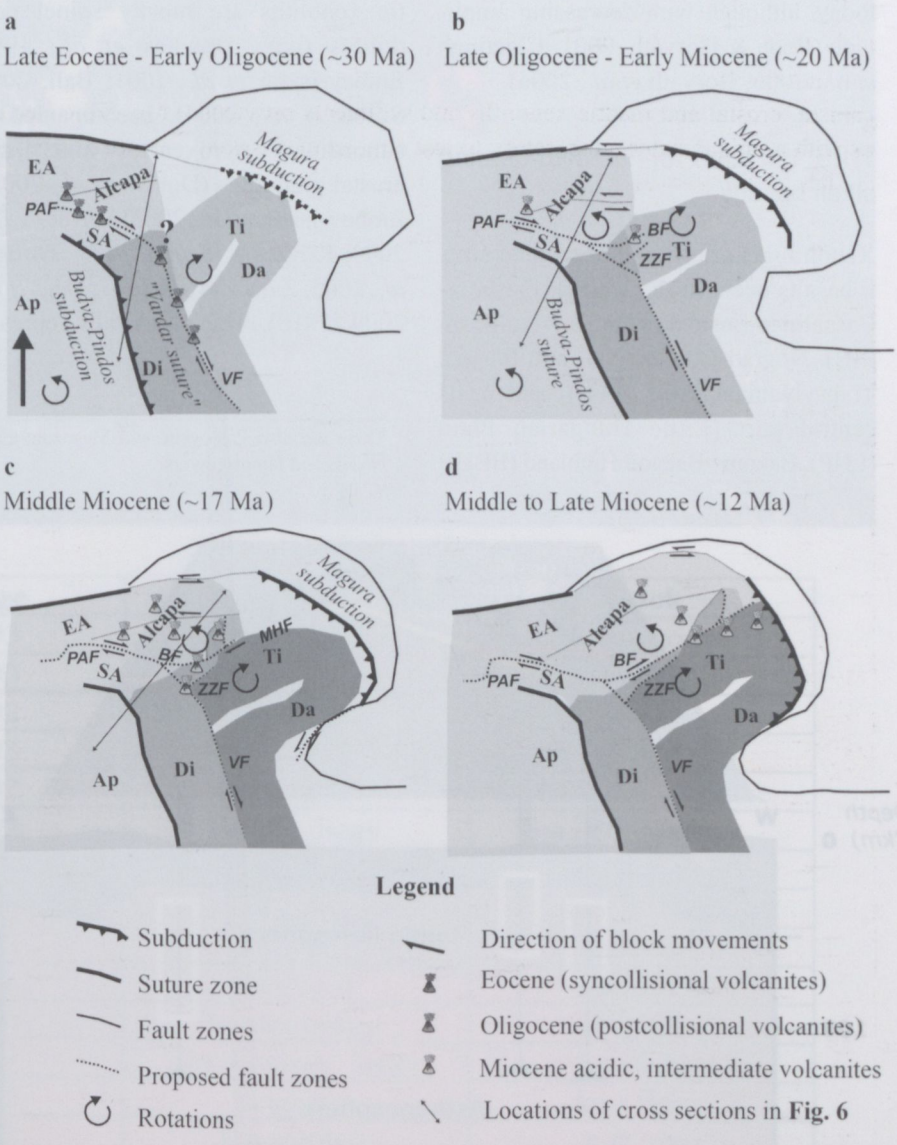

Fig. 2. Schematic summary of major tectonic events in the Carpathian-Pannonian region since the Late Eocene from a "mantle perspective", Kovács & Szabó (2008). Main tectonic features as subduction zones, sutures and faults are indicated on the map. Abbreviations are the followings for tectonic units – EA: Eastern Alps, SA: Southern Alps; Ap: Apulian indenter, Da: Dacia, Di: Dinarides, Ti: Tisza; for tectonic lines – BF: Balaton fault, MHF: Middle-Hungarian fault, PAF: Periadriatic fault, VF: Vardar fault, ZZF: Zagreb–Zemplén fault. Please note that ZZF and MHF is basically the same fault, the northern part of which is called as the MHF. Rotations of the Tisza-Dacia block are only schematic; see Patrascu *et al.* (1994) for further details.

tectonic phase is considered to be driven by the westward subduction of the European margin beneath the internal Carpathian area (Horváth, 1993; Jolivet & Faccenna, 2000) and an eastward directed asthenospheric flow could be also an additional driving force (Kovács & Szabó, 2008). The extrusion and extension of the continental blocks was gradually ceased due to the collision between ALCAPA and the European platform, which started 16 Ma ago, and becomes younger towards the south-east (Fig. 2). This phase still shapes the area today, although with decreasing amplitude (Bada & Horváth, 2001; Cloetingh *et al.*, 2006; Horváth *et al.*, 2006).

1.1.3 Location of xenolith-bearing alkali basalts

Xenolith-bearing Plio–Pleistocene alkali basalts occur at the edge of the Intra-Carpathian Basin System [Styrian Basin (SB), Nógrád-Gömör (NG) and Eastern Transylvanian Basin (ETB)] and in its central part [Little Hungarian Plain (LHP), Bakony–Balaton Highland (BBH)] (Fig. 1, 3)[1]. These xenoliths in alkali basalts are of lithospheric and in some cases asthenospheric origin. Because the eruption of the host alkali basalts postdated the major tectonic events in the CPR, their xenoliths recorded the effects of the preceding events, which include deformation (Falus, 2004; Falus *et al.*, 2000, 2008; Hidas *et al.*, 2007), metasomatism and melt extraction (Bali *et al.*, 2002, 2008b; Szabó *et al.*, 2009; Hidas *et al.*, 2010) and can be used as probes into the evolution of lithospheric block in extensional settings. The upper mantle xenoliths are mostly spinel peridotites (*e.g.*, Downes *et al.*, 1992; Embey-Isztin *et al.*, 2001; Bali, 2004; Szabó *et al.*, 2004), accompanied by subordinate pyroxenites and lower crustal granulites (Dobosi *et al.*, 2003b; Embey-Isztin *et al.*, 2003; Kovács *et al.*, 2004; Kovács & Szabó, 2005; Török *et al.*, 2005; Zajacz *et al.*, 2007; Dégi *et al.*, 2009, 2010). The peridotites represent residual mantle material showing textural and geochemical evidence for a complex history of melting and recrystallization, irrespective of location within the region (Szabó *et al.*, 2004). The mantle xenoliths contain hydrous phases (pargasitic and kaersutitic amphiboles and rarely phlogopite) as evidence for modal metasomatism, in all occurrences of the region (Embey-Isztin, 1976; Szabó *et al.*, 1994, 2004, 2009). The lithospheric mantle sampled as xenoliths is more deformed in the centre of the CPR than towards the edges. At the field trip we will visit the Bakony–Balaton Highland, which is the most well known and studied alkali basaltic volcanic field in the CPR and gives an insight into the central and thinnest part of the lithosphere beneath the CPR.

[1] There are also Paleogene and Mesozoic alkali basalts and lamprophyres.

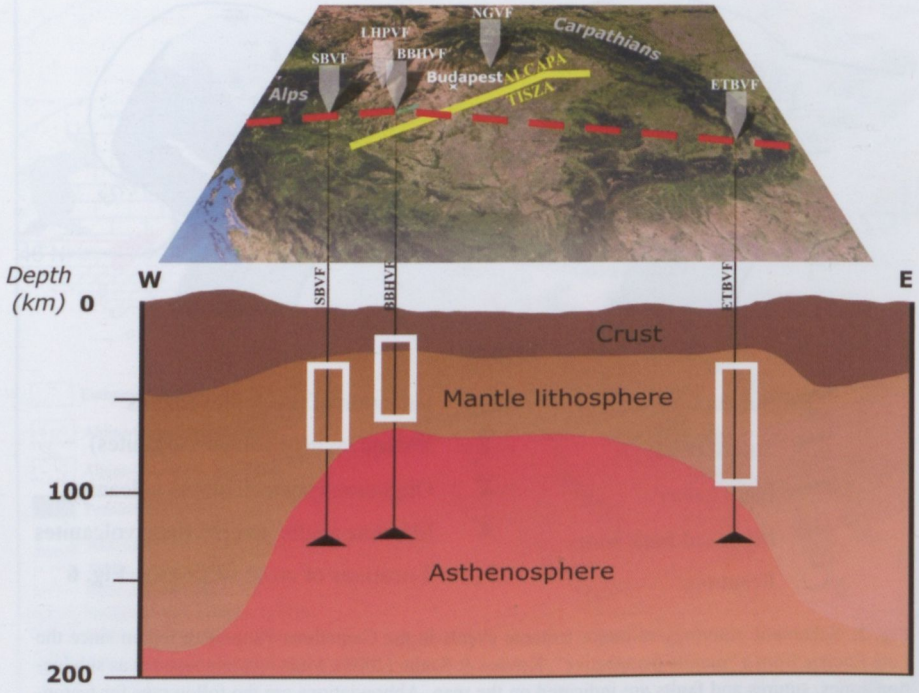

Fig. 3. Schematic block diagram of the Carpathian–Pannonian Region including a W–E cross section of the underlying lithosphere after Lenkey (1999). Major upper mantle xenolith localities in the Plio-Pleistocene alkali basaltic occurrences are also indicated: BBHVF – Bakony–Balaton Highland Volcanic Field; ETBVF – Eastern Transylvanian Basin Volcanic Field; LHPV – Little Hungarian Plain Volcanic Field; NGVF – Nógrád–Gömör Volcanic Field; SBVF – Styrian Basin Volcanic Field.

1.2 Field trip to the Bakony–Balaton Highland Volcanic Field

1.2.1 Geological framework and pre-Neogene basement

The Bakony–Balaton Highland Volcanic Field (BBHVF) is situated in the western Pannonian Basin (western Hungary) on the northern shore of the Lake Balaton (Fig. 4). Geologically, it is a well known and the best-studied young volcanic area on the southern margin of the ALCAPA microplate.

The BBHVF belongs to the Transdanubian Central Range unit (a subunit of the ALCAPA), which is correlated with the Upper Austroalpine nappes of the east Alpine orogen (Majoros, 1983; Kázmér & Kovács, 1985; Tari, 1991). The underlying basement of the volcanic field consists of Paleozoic rocks such as Silurian schist and Permian red sandstone (Császár & Lelkes-Felvári, 1999) and a thick Mesozoic carbonate sequence (Budai & Vörös, 1992; Haas *et al.*, 1999), which were deposited on the Alpine units (SW from their present location) and were transported towards east-northeast by the movement of the ALCAPA microplate during the geodynamic evolu-

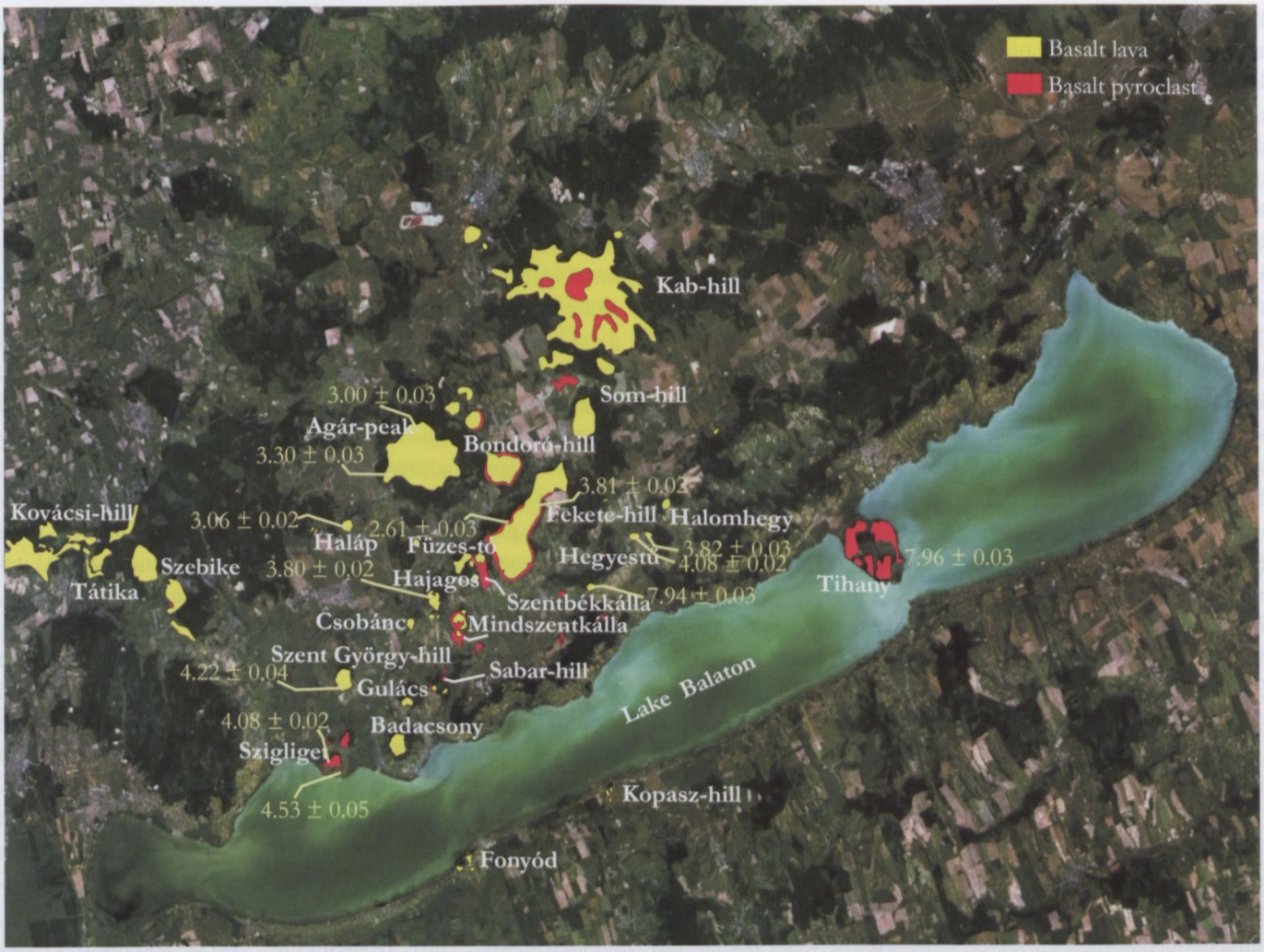

sample no.	Ar-Ar age	Locality	Rock
FT7	2.61±0.03	Füzes-tó	scoria cone
AG-1	3.00±0.03	Agár-tető	shield volcano
HA-1	3.06±0.02	Haláp	maar
AG-2	3.30±0.03	Agár-tető	shield volcano
HAJ	3.80±0.02	Hajagos	maar filling lava lake
FH-4	3.81±0.02	Fekete-hegy	maar filling lava
HAL-2	3.82±0.03	Halomhegy	lava flow
HAL-1	4.08±0.05	Halomhegy	scoria cone
VAR	4.08±0.02	Szigliget	diatreme
HD10	4.12±0.01	Hegyesd	diatreme
SP1861	4.15±0.05	Sümegprága	sill & dike
SztGY	4.22±0.04	Szt. György-hegy	lava lake
SzgD	4.53±0.05	Szigliget	lava flow
KS-1	4.63±0.02	Kissomlyó	tuff ring
TW-13	4.74±0.02	Tótihegy	basanite
SG-2	5.48±0.01	Ság-hegy	tuff
HT-6	7.94±0.03	Hegyestű	lava flow
TIH	7.96±0.03	Tihany	maar

Fig. 4. Basaltic occurrences and Ar-Ar ages in the Bakony–Balaton Highland Volcanic Field (age data from Wijbrans *et al.*, 2007).

tion of the Pannonian Basin. This basement now forms a large-scale anticline structure of Eoalpine origin in the Transdanubian Central Range and is locally covered by Tertiary sediments (Tari *et al.*, 1992; Horváth, 1993). Tertiary sediments were deposited in local sedimentary basins on a regional erosional unconformity (Müller & Magyar, 1992; Müller *et al.*, 1999). In the Neogene, just shortly before the volcanism started, a large lake, the Pannonian Lake, occupied major portion of the Pannonian Basin, which had a very colourful sedimentary environment as reflected in the irregular basin morphology (Kázmér, 1990). The lacustrine sandstones, mudstones, marls of the brackish Pannonian Lake are widespread in the Pannonian Basin (Jámbor, 1980; Gulyás, 2001). Just before volcanism started, the area in the western Pannonian Basin formed an alluvial plain with unconsolidated water saturated sediments in significant spatial and temporal variation (Kázmér, 1990).

1.2.2 The alkali basaltic volcanism

The volcanic centres of the BBHVF were active between 7.96 Ma and 2.61 Ma (Fig. 4) (Balogh *et al.*, 1982; Borsy *et al.*, 1986; Balogh & Pécskay, 2001; Balogh & Németh, 2005; Wijbrans *et al.*, 2007) and produced mostly alkali basaltic volcanic rocks (Szabó *et al.*, 1992; Embey-Isztin, 1993). The BBHVF itself has approximately 50 basaltic volcanoes in a relatively small area (~3500 km^2), however the number of vents maybe far more than 50 due to the existence of volcanic complexes and nested volcanoes (Martin *et al.*, 2003). The alkali basaltic volcanism in the western Pannonian Basin was of a predominantly subaerial, intracontinental type. However, large shallow water bodies may have been present during eruptions, which most likely led to the formation of emergent volcanoes (Kokelaar, 1983; White & Houghton, 2000). After volcanism ceased, fluvial/alluvial sedimentation was widespread in the western Pannonian Basin and major erosion affected the BBHVF, as well (Csillag *et al.*, 1984; Németh *et al.*, 2003). All types of eroded volcanoes can be found in the western Pannonian Basin, including the BBHVF, where the most prominent geomorphologic formations are the circular, lava-capped buttes. These centres are usually related to phreatomagmatic volcanoes, such as maar structures and tuff rings (Németh *et al.*, 2003). Lake Balaton is a recent landform and its history dates back only 17,000–15,000 years (Cserny & Corrada, 1989; Tullner & Cserny, 2003).

1.2.3 Petrography and geochemistry of the alkali basalts

The alkali basalts are remarkably unaltered, moderately porphyritic and holocrystalline, however rarely contain small amounts of glass. The mineralogy is a typical of alkali basalts with assemblages of olivine phenocrysts (Fo_{78-86}) occasionally accompanied by clinopyroxene. The matrix is composed of plagioclase, Ti-rich clinopyroxene, olivine, titanomagnetite rarely coexisting with ilmenite, as well as apatite (Embey-Isztin *et al.*, 1993). Mantle-derived peridotite xenoliths and xenocrysts, as well as lower crustal granulite xenoliths, are frequent at some localities. Major element analyses indicate that the lava rocks are invariably of alkali and sodic character ($K_2O/Na_2O < 1$ wt%). They range in composition from olivine tholeiite to nephelinite, however most are alkali basalt and basanite. The mg# of the BBHVF alkali basalts varies from 54 to 69. This range of mg# indicates that a few lava compositions are primitive, whereas most of them show the effects of moderate fractional crystallization (Szabó *et al.*, 1992; Embey-Isztin *et al.*, 1993).

The trace element composition of the BBHFV alkali basalts resemble closely OIB (*e.g.*, Embey-Isztin *et al.*, 1993; Seghedi *et al.*, 2004a) and differs from that in the Perşani (Persányi) Mts. (Eastern Transylvanian Basin), where a subduction affected source can be identified (Downes *et al.*, 1995; Seghedi *et al.*, 2004b) (Fig. 3). It is significant from the geodynamic point of view that the Perşani Mts. basalts were erupted contemporaneously with calc-alkalinene and adakite-like calc-alkaline and shoshonitic magmas (Seghedi *et al.*, 2004a), between 1.5 and 0.5 Ma (Panaiotu *et al.*, 2004).

Isotopic ratios of $^{87}Sr/^{86}Sr$, $^{143}Nd/^{144}Nd$, $\delta^{18}O$, δD, and Pb span the range of Neogene alkali basalts from western and central Europe (Wilson & Downes, 1991), and suggest that the magmas of the BBHFV alkali basalts were dominantly derived from asthenospheric partial melting, however Pb isotopes indicate that in most cases they were modified by melt components from the enriched lithospheric mantle through which they have ascended (Embey-Isztin *et al.*, 1993; Embey-Isztin & Dobosi, 1995; Harangi *et al.*, 1995; Dobosi *et al.*, 1998; Harangi, 2001; Dobosi *et al.*, 2003a; 2003b). $\delta^{18}O$ values indicate that the magmas have not been significantly contaminated with crustal material during ascent, and isotopic and trace-element ratios therefore reflect mantle source characteristics. Incompatible-element patterns show that the basic lavas erupted in the western Pannonian Basin, including the Bakony–Balaton Highland, are relatively homogeneous and are enriched in K, Rb, Ba, Sr, and Pb (Embey-Isztin *et al.*, 1993; Dobosi *et al.*, 1998). Primitive mantle-normalized trace element patterns indicate a general increase of incompatible trace element abundances.

In addition, $^{207}Pb/^{204}Pb$ is enriched relative to $^{206}Pb/^{204}Pb$. In these respects, the lavas of the Bakony–Balaton Highland area differ from those of other regions of Neogene alkali magmatism of Europe. This may be due to the introduction of marine sediments into the mantle during the earlier period of subduction and metasomatism of the lithosphere by slab-derived fluids rich in K, Rb, Ba, Pb, and Sr (Embey-Isztin *et al.*, 1993).

1.2.4 Petrography and geochemistry of upper mantle xenoliths

Ultramafic xenoliths can be found in basanitic lava flow and pyroclastic volcanic products at six locations (Tihany, Bondoró Hill, Füzes-tó, Szentbékkálla, Mindszentkálla,

Szigliget) (Fig. 5). Most of the xenoliths are spinel lherzolites, however harzburgite, clinopyroxenite, orthopyroxenite, wehrlite, websterite and, sometimes, composite xenoliths appear, too. The most frequent texture type is equigranular (Embey-Isztin *et al.*, 1989; Downes *et al.*, 1992; Downes & Vaselli, 1995; Szabó *et al.*, 1995a, 2004), whereas protogranular and porphyroclastic xenoliths could be found in smaller portion. Special textures like poikilitic, flattened equigranular, and mylonitic are also present in xenoliths in highly different portion on locations (Figs. 5, 6). The peridotite xenoliths from alkali basalts of the Bakony–Balaton Highland have a bulk compositions ranging from 37 to 45 wt% MgO, 1.0 to 3.5 wt% CaO, and Al_2O_3, and 0.02 to 0.14 wt% TiO_2 (Fig. 7). There are no significant chemical differences of xenoliths among the major localities, although the compositional range of the Nógrád-Gömör Volcanic Field covers the highest MgO-bearing xenoliths, whereas ranges of the Styrian Basin and Eastern Transylvanian Basin Volcanic Fields xenoliths involve samples containing the lowest MgO content. Concentration of basaltic elements, representing Al_2O_3 and TiO_2, and of CaO displays a negative correlation with MgO (Fig. 7) as Downes & Vaselli (1995) have already noted. These chemical features of the CPR xenoliths are in agreement with xenoliths from other localities (*e.g.*, Rhenish Massive, Massif Central) and with Alpine massive peridotites (Bodinier *et al.*, 1988; Downes *et al.*, 1991; Wilson & Downes, 1991). It is suggested that gradual depletion in basaltic elements is connected at first consideration to partial melting event(s). The most frequent mineral is olivine in these xenoliths with mg# and Fo content between 89 and 92 along with low CaO content (0.04–0.11 wt%). Al_2O_3 content of orthopyroxenes is generally higher in protogranular xenoliths than in porphyroclastic or equigranular ones. In most cases, clinopyroxene is Cr-diopside with mg# between 89 and 93. The spinel composition is the most variable with cr# between 10 and 55 and mg# between 80 and 60 (Embey-Isztin *et al.*, 1989; Downes *et al.*, 1992; Szabó *et al.*, 1995a). Additional mineral phase can be pargasitic amphibole (Embey-Isztin, 1976; Bali *et al.*, 2002; Szabó *et al.*, 2004). The clinopyroxenes from protogranular xenoliths from the Bakony–Balaton Highland are LREE-depleted

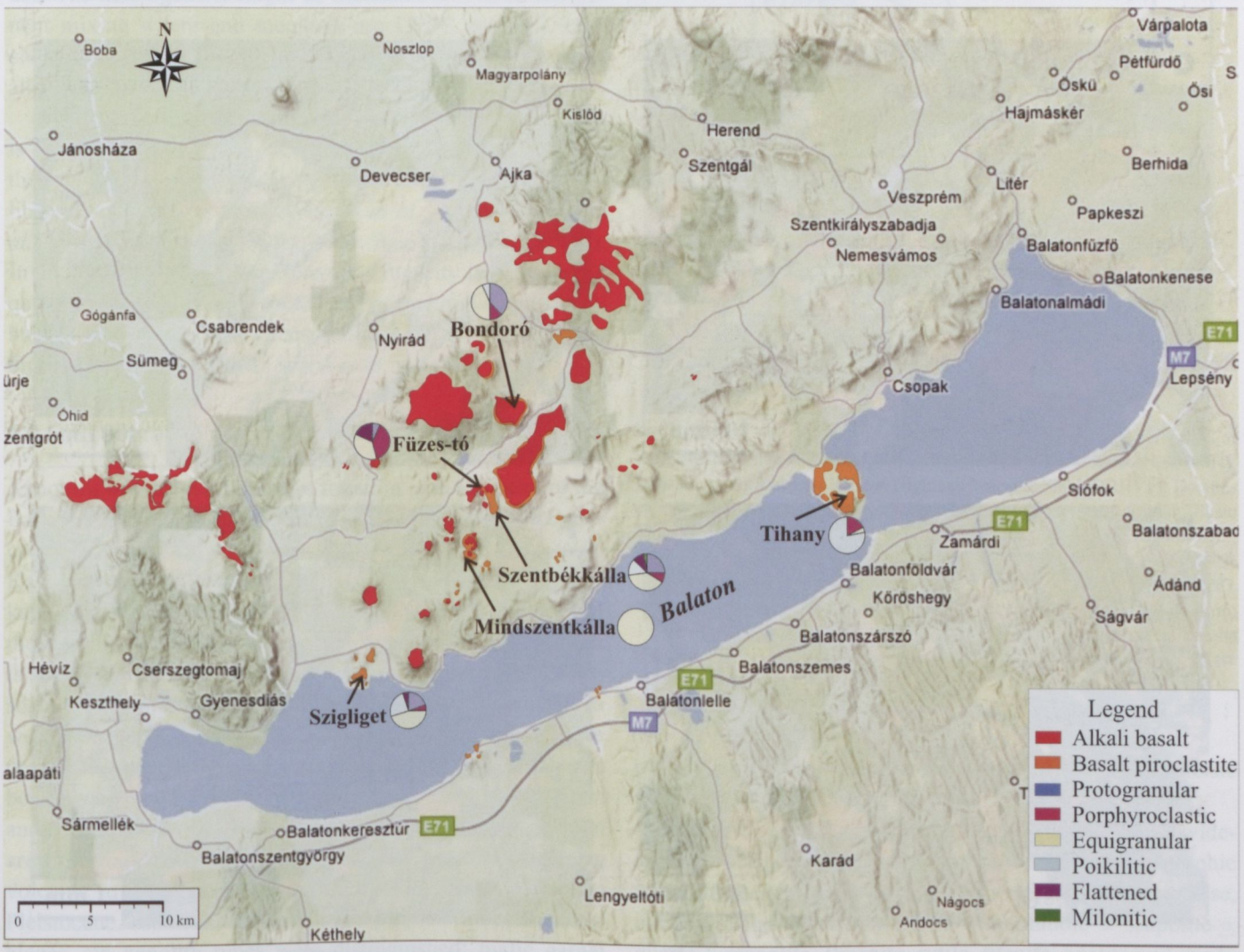

Fig. 5. Occurrence of upper mantle xenoliths in the Bakony–Balaton Highland Volcanic Field. The map is based on Jugovics (1971) and Harangi (2001).

which is characteristic for undeformed subcontinental lithospheric mantle, whereas xenoliths with porphyroclastic and equigranular texture contain clinopyroxenes, which are LREE-enriched. This enrichment could be the result of a metasomatic event related to deformation (Downes *et al.*, 1992). The $^{87}Sr/^{86}Sr$ values of separated clinopyroxenes from Bakony–Balaton Highland xenoliths vary between 0.70307 and 0.70523, the $^{143}Nd/^{144}Nd$ ratio ranges from 0.513341 to 0.512733 (Fig. 8). The ε_{Nd} values of clinopyroxenes from protogranular xenoliths are the highest, whereas porphyroclastic and equigranular xenoliths show lower values. Clinopyroxenes from protogranular xenoliths have high Sm/Nd and $^{143}Nd/$

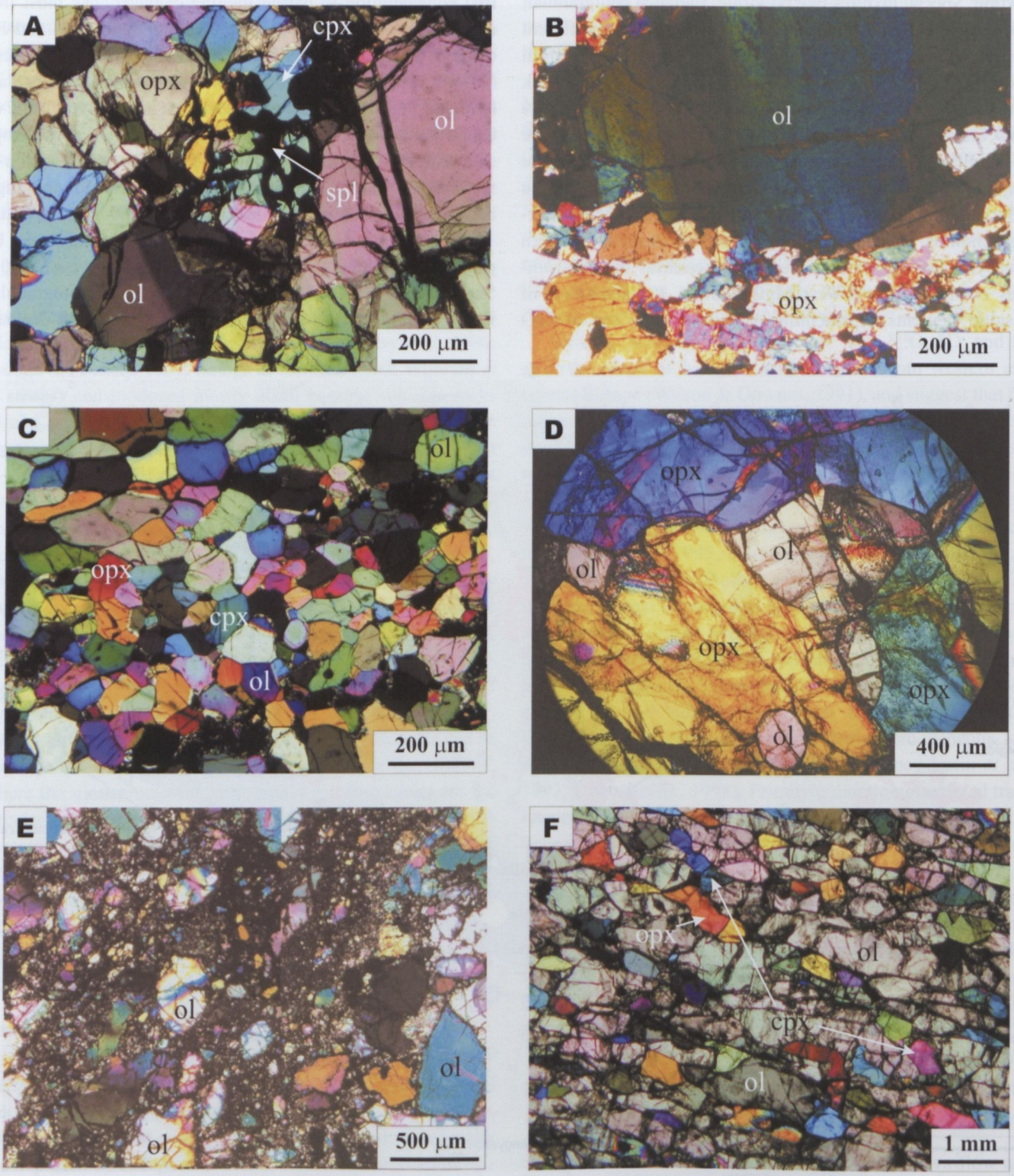

Fig 6. Textural types of ultramafic xenoliths from the Bakony–Balaton Highland Volcanic Field: A) protogranular, B) porphyroclastic, C) equigranular, D) poikilitic, E) milononitic, D) flattened equigranular. Abbreviations: ol – olivine, opx – orthopyroxene, cpx – clinopyroxene, spl – spinel.

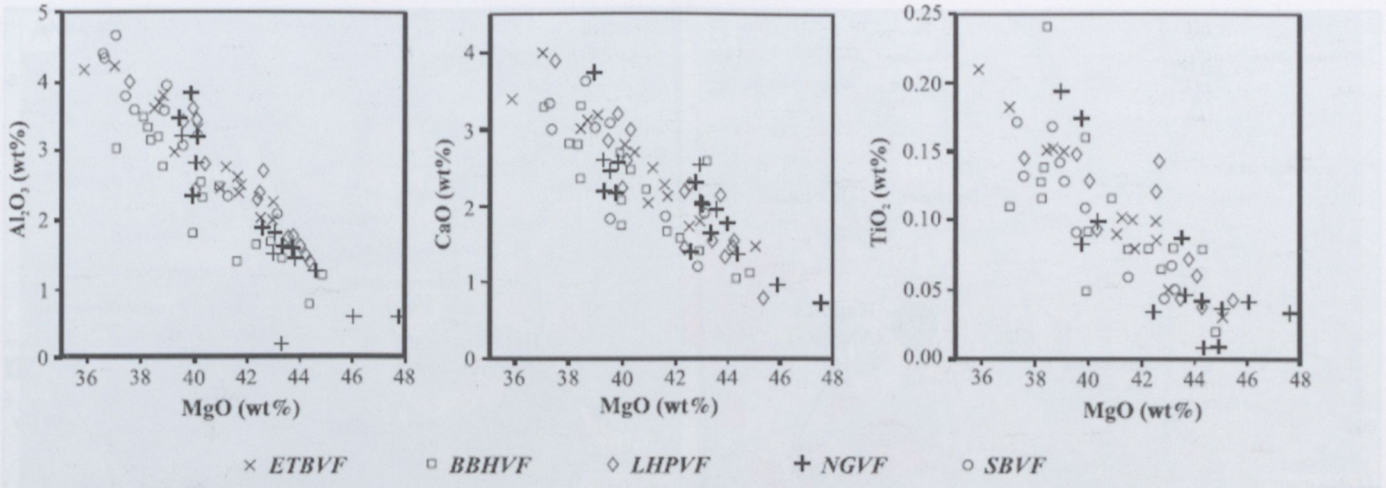

Fig. 7. Harker diagrams of bulk compositions of the Carpathian-Pannonian Region ultramafic xenoliths for TiO_2, Al_2O_3, CaO vs. MgO (Szabó *et al.*, 2004). Data source for the Bakony–Balaton Highland Volcanic Field (BBHVF): Embey-Isztin *et al.* (1989) and Downes *et al.* (1992). For comparison, ultramafic xenoliths from Styrian Basin Volcanic Field (SBVF) (Kurat *et al.*, 1991 and Vaselli *et al.*, 1996), from Little Hungarian Plain Volcanic Field (LHPVF) (Embey-Isztin *et al.*, 1989; Downes *et al.*, 1992 and Szabó *et al.*, 1995b), from Nógrád–Gömör Volcanic Field (NGVF) (Szabó & Taylor, 1994) and from Eastern Transylvanian Basin Volcanic Field (ETBVF) (Vaselli *et al.*, 1995).

^{144}Nd values, whereas equigranular samples show lower values. The heterogeneity might be the result of a three component mixing where end members are LREE depleted, high εNd low εSr mantle; Pliocene alkali basalts and Miocene calc-alkali magmas (Fig. 8) (Downes *et al.*, 1992).

The equilibrium temperature of BBHVF mantle xenoliths is between 880 and 1090 °C. Protogranular peridotites have the highest and equigranular xenoliths have the lowest equilibrium temperatures (Embey-Isztin *et al.*, 1989; Downes *et al.*, 1992; Szabó *et al.*, 1995a, 2004; Bali *et al.*, 2002, 2007). In most cases the equilibrium oxygen fugacity is between the quartz-fayalite-magnetite (QFM) and magnetite-wüstite (MW) buffers, but the secondary recrystallized peridotites show the highest value above QFM (Szabó *et al.*, 1995a).

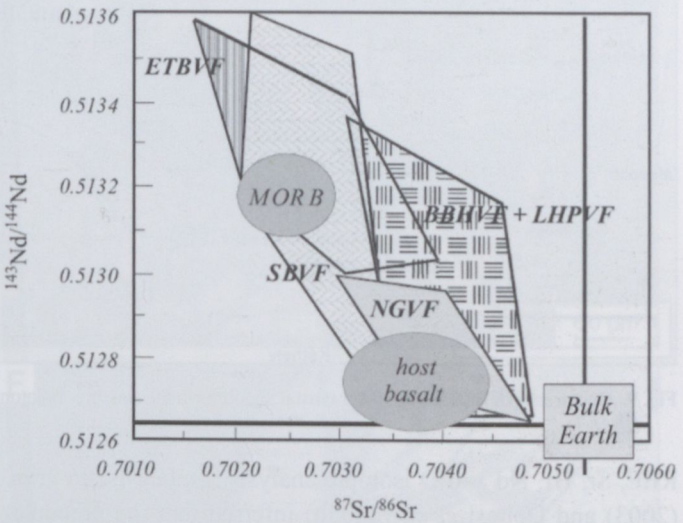

Fig. 8. The Sr and Nd isotopic compositions of separated clinopyroxenes of the Carpathian-Pannonian Region ultramafic xenoliths (Szabó *et al.*, 2004). Data source for Bakony–Balaton Highland Volcanic Field (BBHVF): Downes *et al.* (1992). For comparison, ultramafic xenoliths from Styrian Basin Volcanic Field (SBVF) (Vaselli *et al.*, 1996 and Bali & Szabó, unpublished), from Little Hungarian Plain Volcanic Field (LHPVF) (Downes *et al.*, 1992) from Nógrád–Gömör Volcanic Field (NGVF) (Szabó & Vaselli, unpublished), and from Eastern Transylvanian Basin Volcanic Field (ETBVF) (Vaselli *et al.*, 1995). Also, for comparison, the isotopic compositions of the host basalts (Embey-Isztin *et al.*, 1993), MORB and bulk earth (Zindler & Hart, 1986) are also shown.

1.2.5 Petrography and geochemistry of crustal xenoliths

Xenoliths of crustal origin were found in nine localities of the Bakony–Balaton Highland Volcanic Field (BBHVF): Badacsony, Balatoncsicsó (*Fenyves-hegy*), Kapolcs (*Áldozó-tető*), Kapolcs (*Nagy-tó*), Káptalantóti (*Sabar-hegy*), Mindszentkálla, Szentbékkálla, Szigliget, Tihany (Fig. 9). In general they contain a peak metamorphic mineral assemblage, which is usually overprinted by post-peak mineral assemblages to some extent. Most peak metamorphic mineral assemblages were formed in an overthickened crust during the Alpine orogeny. Some post-peak mineral assemblages and fluids can be assigned to crustal evolution during the Miocene extrusion and extension of the ALCAPA block, whereas some of them are the products of xenolith – host melt interaction during volcanic transportation to the surface in the Pliocene–Pleistocene. Based on the peak metamorphic mineral assemblages, six xenolith types were distinguished: mafic garnet granulites, metapelitic granulites, garnet-orthopyroxene-plagioclase felses, clinopyroxene-plagioclase felses, felsic granulites and buchites.

1) Mafic garnet granulites (Fig. 10a) are the most widespread crustal xenoliths in the region. The peak metamorphic mineral assemblage usually consists of garnet, plagioclase, clinopyroxene ± orthopyroxene ± amphibole ± scapolite ± quartz ± scapolite. Ilmenite, rutile, titanite, apatite and rarely zircon are observable as accessory phases. On the basis of

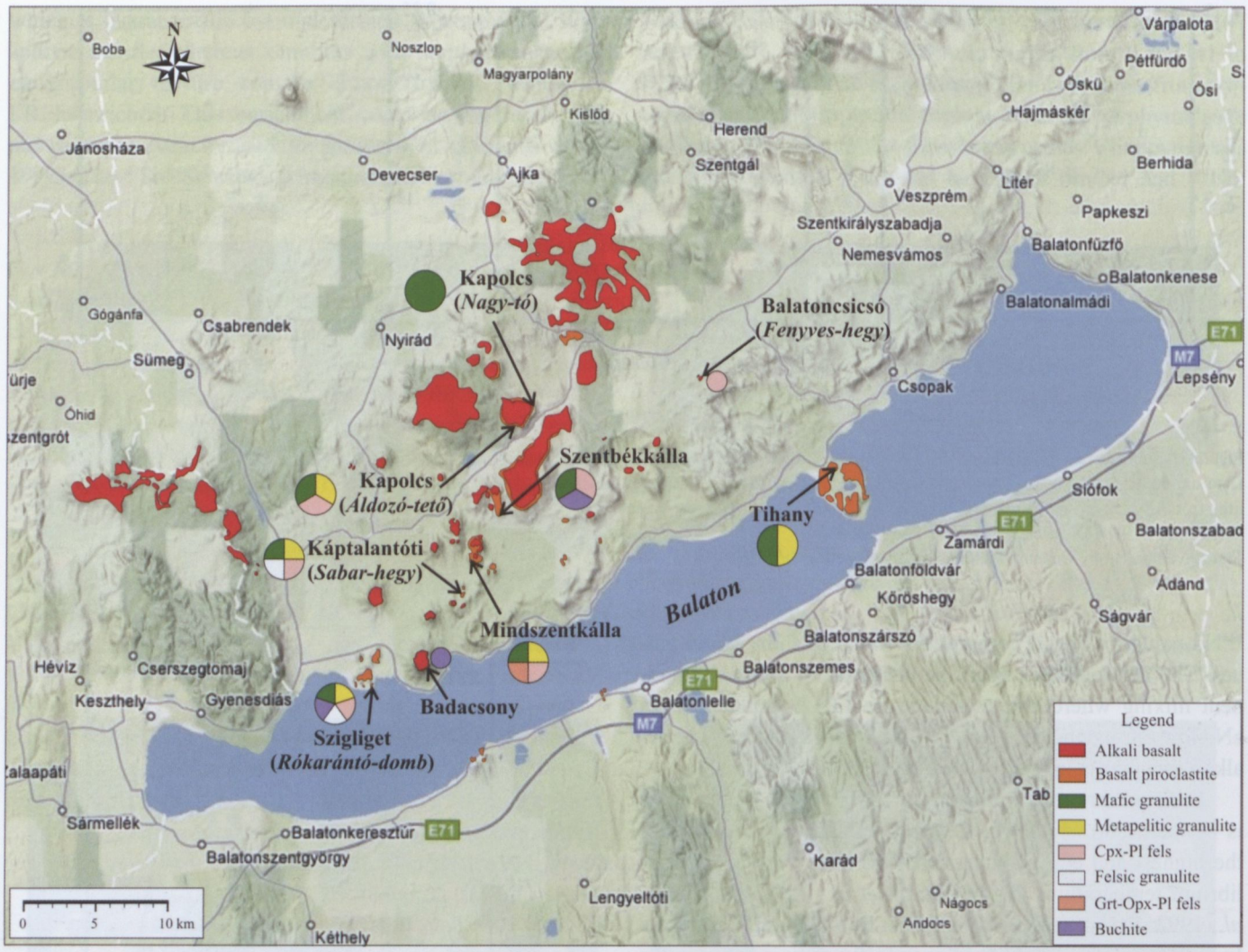

Fig. 9. Occurrence of middle and lower crustal xenoliths in the Bakony–Balaton Highland Volcanic Field. The map is based on Jugovics (1971) and Harangi (2001).

REE, Sr, Hf, Nd and O isotopic analysis, Embey-Isztin *et al.* (2003) and Dobosi *et al.* (2003b) inferred that the precursor rock of the mafic garnet granulites might have been oceanic pillow basalts with primitive mafic to slightly tholeiitic liquid composition. Detailed geothermobarometric analysis of the peak metamorphic mineral assemblage in large number xenoliths has shown that a complete lower crustal section between 1–1.6 GPa (35–57 km) and 750–1070 °C have been sampled. The calculated equilibrium pressures and temperatures define a paleogeotherm with a steepness of 15 °C/km. This corresponds to the pre-extensional lower crust in the overthickened Alpine orogenic root (Dégi, 2009). At this stage of the metamorphic evolution reduced $CO_2 \pm CO \pm C \pm H_2S$ primary fluid inclusions of high density were captured in plagioclase grains (Török *et al.*, 2005). Tectonic processes during the Miocene extrusion/extension of the ALCAPA block were accompanied by several changes recorded in the xenoliths. The activation of fluid channels resulted in the formation of secondary fluid generations with more and more oxidized compositions from $CO_2 \pm CO \pm C$ to $CO_2 \pm CO \pm N_2$ associated with decreasing density (Török *et al.*, 2005). The interaction of percolating fluids and melts with phases of the peak metamorphic mineral assemblage led to the formation of melt pockets and to the exsolution of Fe-Ti oxides by reduction (Dégi *et al.*, 2009). Significant decompression led to the breakdown of garnets to submicron-sized symplectites of Al-rich orthopyroxene, spinel and anorthite (Dégi *et al.*, 2010). The xenolith–host melt interaction during volcanic transportation to the surface sometimes significantly modified the microstructures and chemical compositions of minerals formed during crustal evolution, although its duration did not exceed a day (Dégi *et al.*, 2009, 2010). The formation of low-density pure CO_2 fluid inclusions in plagioclase and clinopyroxene is also related to this process.

2) Metapelitic granulites are less abundant. Sometimes they are found in composite xenoliths in sharp contact with mafic garnet granulites. Based on their mineralogical composition, two groups of metapelitic granulites were distinguished. Metapelites of the first group contain predominant garnet and sillimanite with subordinate quartz and plagioclase (Fig. 10b). Corundum, hercynitic spinel, biotite, K-feldspar may also occur as accessory phases. The mode of garnet and

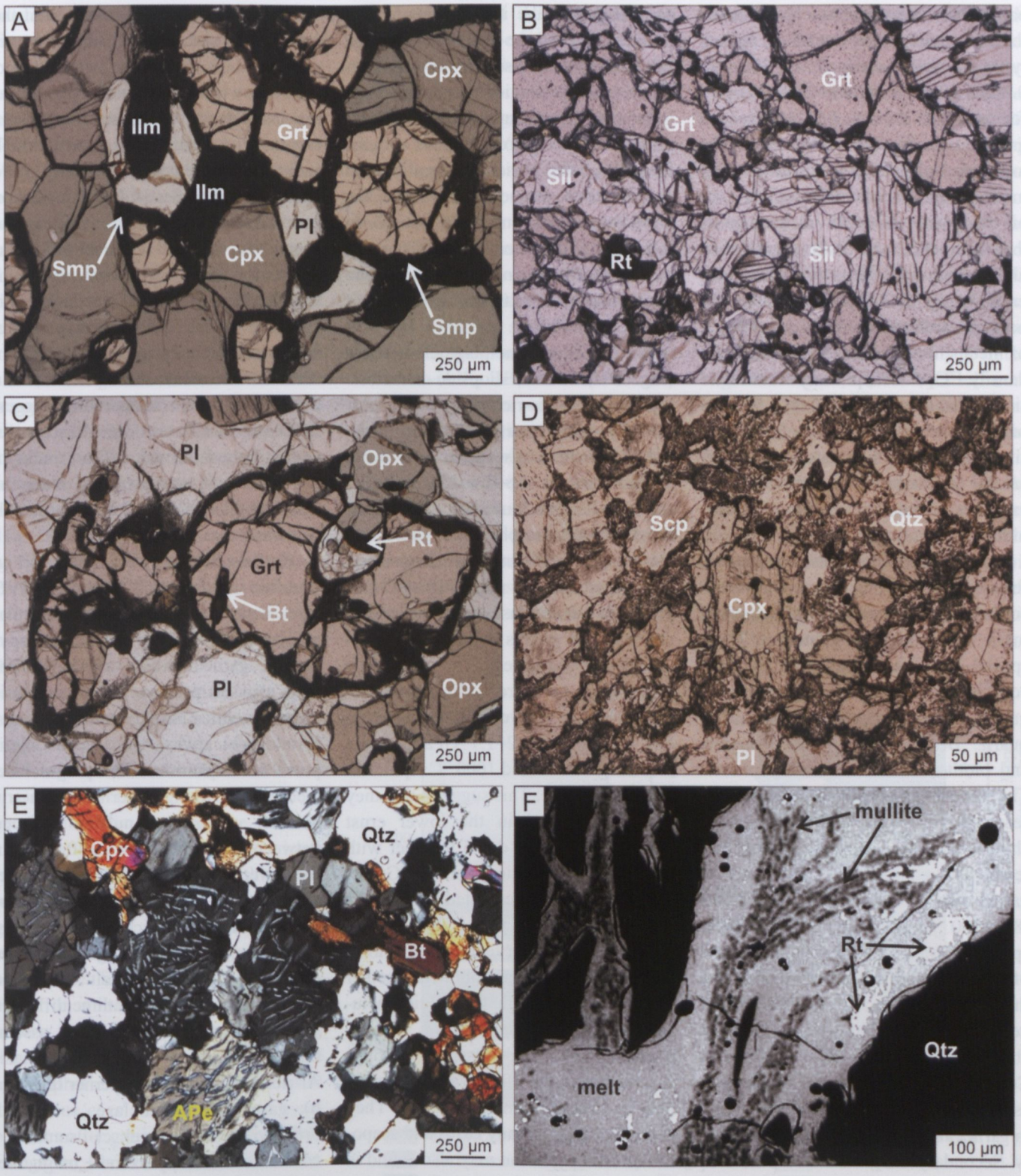

Fig. 10. Crustal xenoliths from the Bakony–Balaton Highland Volcanic Field. A) Mafic garnet granulite. B) Metapelitic granulite. C) Garnet-orthopyroxene-plagioclase fels. D) Low-pressure clinopyroxene-plagioclase fels. E) Felsic granulite. F) Buchite-containing mullite pseudomorph after muscovite. Abbreviations: Ape – antiperthite, Bt – biotite, Cpx – clinopyroxene, Grt – garnet, Ilm – ilmenite, Opx – orthopyroxene, Pl – plagioclase, Qtz – quartz, Rt – rutile, Scp – scapolite, Sil – sillimanite, Smp – symplectite after garnet.

sillimanite is usually close to 90–95 vol%, rarely it can be as low as 60 vol% which is associated with the increase of biotite and plagioclase content. This suggests that these metapelites are restites and significant amount of partial melt was extracted from the pelitic precursors. Plagioclase–garnet felses are found in the second group. They usually contain corundum, spinel, orthopyroxene, ilmenite, rutile, biotite and quartz in minor amounts besides plagioclase and garnet. Geothermo-

barometric investigations have shown that the equilibration conditions of both types of metapelites (740–950 °C, 0.9–1.2 GPa and 890–910 °C, 1.0 GPa for xenoliths of the first and second group, respectively) correspond to the lower crustal geotherm constructed for mafic garnet granulites. The occurrence of composite xenoliths also suggests that metapelitic and mafic garnet granulites were both formed in the lower crust during the Alpine orogenesis. The peak metamorphic mineral assemblage of metapelitic granulites contains high-density $CO_2 \pm CH_4$ primary fluid inclusions. The formation of $CO_2 \pm N_2$ secondary fluid inclusions with lower density may also be associated with lower crustal evolution during the extrusion/extension of the ALCAPA block.

3) Garnet-orthopyroxene-plagioclase felses (Fig. 10c) are usually found in composite xenoliths on the contact of mafic and metapelitic granulites. These special rocks are dominated by non-equilibrium microstructural domains of garnet, orthopyroxene, plagioclase ± quartz. Besides these, rutile, ilmenite and biotite occur as accessory phases. The modal proportion of garnet may reach 60 vol% and some garnet grains show concentric chemical zoning patterns. The equilibration conditions of garnet-orthopyroxene-plagioclase felses (880–900 °C and 1.2–1.3 GPa) correspond with the equilibration conditions of the contacting rocks within error and they fit well to the Alpine lower crustal geotherm. Fluid inclusions are the most abundant in this xenolith type. Primary $CO_2 \pm N_2$ and pure CO_2 fluid inclusions associated with biotite relics are found in garnet and orthopyroxene, respectively. Secondary CO_2 + CO and pure CO_2 fluid inclusions occur in plagioclase and garnet, respectively. Microstructural and mineral chemical characteristics of garnet-orthopyroxene-plagioclase felses as well as their fluid content suggest that these rocks went through CO_2-rich fluid associated partial melting of biotite and quartz-bearing domains and the observed non-equilibrium microstructures were formed due to the interaction of these partial melts and the wall rock. The lack of K-bearing phases in the garnet-orthopyroxene-plagioclase felses suggests that significant amount of melt was extracted from these rocks. Regarding the preserved equilibration pressure and temperature values, the partial melting event could have been induced by formation of fluid channels due to deformation processes at the beginning of the extrusion/extension of the ALCAPA block.

4) Clinopyroxene-plagioclase felses (Fig. 10d) contain diopside–hedenbergite and anorthite-rich plagioclase occasionally with quartz. Besides these, orthopyroxene and scapolite may occur as major phases. Fe-Ti oxides, graphite and titanite are found as accessories. Rarely pseudomorphs after garnet are observed, which consist of plagioclase, clinopyroxene ± magnetite. Clinopyroxene-plagioclase geobarometry defines three groups within clinopyroxene-plagioclase felses.

a) High-pressure clinopyroxene-plagioclase felses were formed between 1–1.4 GPa and 1.2–1.7 GPa pressure assuming 800 °C and 1000 °C equilibration temperature. This suggests that they were also found in the lower crust between 35–60 km depth together with mafic and metapelitic granulites. Garnet pseudomorphs are restricted to xenoliths of this group. Only pure CO_2 fluids are observed as primary fluid inclusions, but all of them re-equilibrated together with secondary pure CO_2 fluid inclusions during the extension.

b) Intermediate-pressure clinopyroxene-plagioclase felses are characterized by magmatic microstructure. They contain quartz in many cases and scapolite or orthopyroxene may also found in them. Assuming 800 °C equilibration temperature, these rocks were formed between 0.5–0.8 GPa. They contain primary and secondary pure CO_2 fluid inclusions, which preserved the same equilibration pressure. Based on these, intermediate-pressure clinopyroxene-plagioclase felses may have formed between 20–28 km depth by the crystallization of felsic-neutral magmas at the lowermost part of the Alpine upper crust.

c) Low-pressure clinopyroxene-plagioclase felses are skarns. They contain meionitic scapolite (Fig. 10d), which indicates high-temperature (900 °C) and low-pressure (0.3–0.4 GPa) formation conditions. They contain primary and secondary very CO_2-rich fluid inclusions occasionally with some H_2S content. Isochors of all fluid inclusions indicate the same equilibration pressure, which corresponds to 8–11 km depth. Mineral chemical characteristics and high equilibration temperature suggest that these rocks were formed by contact metamorphosis of calc-silicate rocks in the upper crust most probably due to the Pliocene–Pleistocene alkali basaltic volcanism.

5) Felsic granulite xenoliths (Fig. 10e) are rarely found in the BBHVF. They mainly consist of quartz and plagioclase, but clinopyroxene, orthopyroxene, garnet, biotite and K-feldspar may also be present. Relic magmatic microstructures dominate these rocks. K-feldspar always occurs as anti-perthitic exsolution in plagioclase. According to geothermobarometric studies, felsic granulites formed between 750–850 °C and 0.5–0.6 GPa in the lowermost part of the Alpine upper crust together with Cpx-Pl felses by the crystallization of felsic-neutral magmas.
6) Buchite xenoliths (Fig. 10f) contain quartz and abundant melt veins and pools. The melt contains three different, very high temperature mineral assemblages: a) mullite + corundum + spinel + Al-rich orthopyroxene ± terner feldspar; b) garnet + plagioclase + Al-rich orthopyroxene + spinel; c) osumilite + cordierite + orthopyroxene + magnetite. The presence of fluid inclusions is restricted to "type a" buchites, where primary low-density CO_2-rich fluid inclusions occur in quartz and high-density, low-salinity H_2O–NaCl or CO_2–H_2O–NaCl fluid inclusions are found in melt. Decreasing water content from the H_2O-oversaturated "type a" buchites to the H_2O-poor "type c"

buchites explains the formation of different mineral parageneses in the three buchite types. Based on feldspar thermometry, fluid densities and the observed mineralogy, buchites were formed by ultrahigh temperature (900–1100 °C) contact metamorphism of quartz and feldspar-rich low- to medium-grade metamorphic rocks containing mica, between 0.2–0.3 GPa pressure in 12–14 km depth of the upper crust, most probably due to the Pliocene–Pleistocene alkali basaltic volcanism.

Detailed petrography, fluid inclusion studies and geothermobarometric studies of crustal xenoliths from the BBHVF allowed to reconstruct the schematic structure of the overthickened Alpine orogenic root prior to the extrusion/extension of the ALCAPA block (Fig. 11a). The upper crust is assumed to be an undivided body, which extends to 28–35 km depth. The intrusion of felsic-neutral magmatic bodies to the lowermost part of the upper crust during the Alpine orogeny resulted in the formation of felsic granulites and quartz-bearing intermediate-pressure clinopyroxene-plagioclase felses. The lower crust extended from 35–60 km depth and it was characterized by a 15 °C/km paleogeotherm. The temperature at the crust/mantle boundary might have reached 1100 °C. This overthickened lower crust mainly consisted of mafic garnet granulites, but metapelitic granulites and high-pressure clinopyroxene-plagioclase felses were also present. Based on mineral stabilities, the lithospheric mantle may have been 30–60 km thick at this tectonic stage. This suggests a lithospheric thickness of about 90–120 km (Falus *et al.*, 2007) based on symplectites after garnets found at the Little Hungarian Plain area not far from the BBHVF. During deformation processes at the beginning of the Miocene extrusion/extension of the ALCAPA block, fluid-induced partial melting took place due to the reactivation of fluid channels, which resulted in the formation of garnet-orthopyroxene-plagioclase felses at the contact of mafic and metapelitic granulites. Equilibration conditions of these rocks suggest that the paleogeotherm remained undisturbed at this stage of the metamorphic evolution. In the later stages of the extrusion/extension of the ALCAPA block, significant crustal thinning to 28–32 km (Fig. 11) took place, which resulted in decompression-induced processes, such as the breakdown of garnet in mafic garnet granulites. The migration of different fluids and melts in the lower crust were continuous during the Miocene crustal evolution and it induced several metasomatic reactions. Post-extensional alkali basaltic volcanism in the BBHVF led to the formation of buchites and low-pressure clinopyroxene-plagioclase felses in the upper crust due to high to ultrahigh temperature contact metamorphism. Precursors of these rocks indicate that low- and medium-grade metamorphic rocks are found beneath the sedimentary sequence in the present day upper crust. Based on mineral stabilities, the post-extensional mafic lower crust should consist of olivine–plagioclase granulites up to 25 km depth and clinopyroxene–plagioclace ± orthopyroxene granulites between 25–32 km depth. The majority of the present-day lithospheric mantle is in the spinel peridotite–spinel pyroxenite stability field, and the thickness of the present-day lithosphere is 60–70 km based on peridotite xenoliths and geophysical surveys (Falus *et al.*, 2000; Horváth *et al.*, 2006). In the previous sections we have shown that Neogene alkali basalt of the Bakony–Balaton Highland Volcanic Field by itself contributed a lot to the better understanding of the geological history of the Pannonian Basin and besides, played a key role in the understanding of the composition and evolution of the deep lithosphere by transporting deep lithospheric xenoliths to the surface. In this section we step away from the large-scale geological processes and the geodynamic

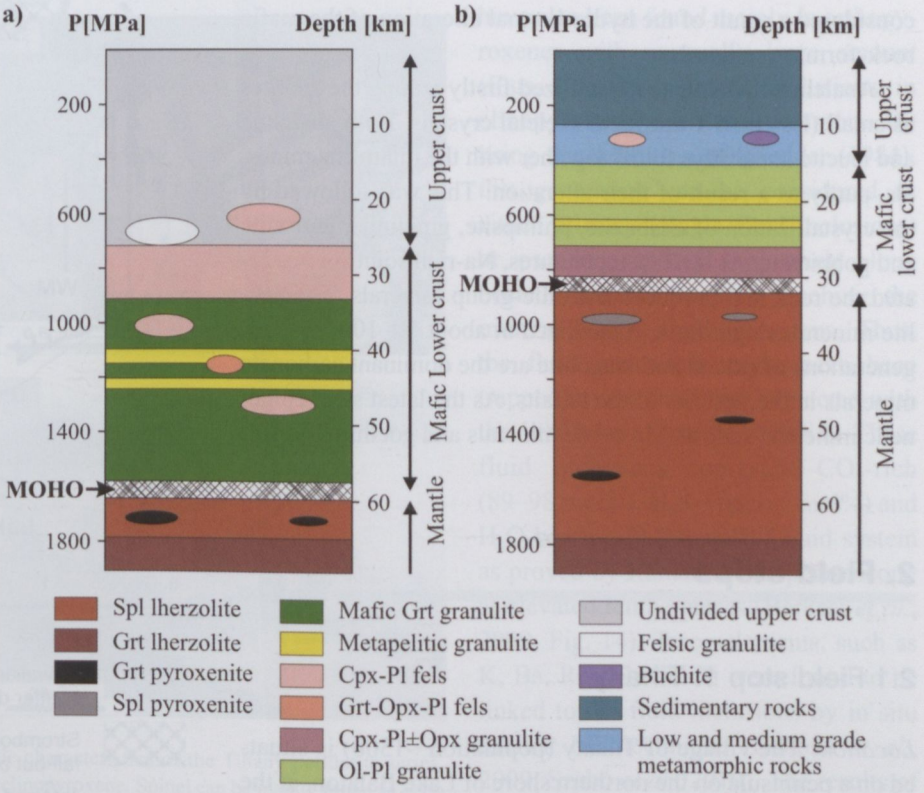

Fig. 11. a) Lithosphere stratigraphy of the pre-Miocene overthickened Alpine orogenic root based on geothermobarometry of crustal xenoliths found in the Bakony–Balaton Highland Volcanic Field (BBHVF) (Török *et al.*, 2005; Dégi *et al.*, 2009; 2010). b) Lithosphere stratigraphy beneath the present day Central Pannonian Basin on the basis of geophysical data (CEL08 profile, unpublished, Celebration2000 working group), mineral equilibria and metamorphic evolution of crustal xenoliths found in the BBHVF (Török *et al.*, 2005; Dégi *et al.*, 2010).

approach to shed light on a tiny (in size), but peculiar (in mineralogical sense) increment of the alkali basalts in the Bakony–Balaton Highland Volcanic Field. Zeolitic mineral assemblage in basalts from this volcanic field has been in the focus of scientific interest in the last two decades. Studies focusing on a restricted area or on selected mineral groups contributed notably to the better knowledge of the mineral paragenesis of this area. However, comprehensive studies on the whole volcanic field has been carried out only in the past few years (Kónya, 2009). As a result, numerous new mineral species has been firstly described from Hungary (*e.g.*, chabazite-Na, phillipsite-Na, gonnardite; Kónya, 2009). In addition, chabazite-Mg was also found and described (Prága Hill, Bazsi, Montagna *et al.*, 2010), which, being a newly described zeolite-group mineral, has an importance to specific mineralogy. The precipitation of the cavity-filling minerals proceeded in many steps. At the wall of the cavities firstly the primary miarolitic mineral phases (sanidine, nepheline, augite, apatite, biotite, ilmenite, hematite, sodalite, magnetite) crystallized, followed by the precipitation of the hydrothermal phases, such as clay minerals, zeolites and carbonates. Clay mineral formation on the crystals of miarolitic minerals can be regarded as generally observed phenomena. These clay minerals are mainly smectites: dominantly saponite, rarely nontronite. Chlorites or mixed-layer clay minerals (chlorite/smectite, illite/chlorite) also occur in small amounts. Their formation is considered a result of the hydrothermal alteration of the mafic rock-forming minerals.

Analcime and leucite crystallized firstly among the zeolites as small (less than 1 mm) and skeletal crystals. Both analcime and leucite are always found together with the miarolitic minerals, partly as a result of their alteration. This was followed by the crystallization of chabazite, phillipsite, gmelinite, garronite and gobbinsite. At lower temperatures, Na-rich solution permeated the rock and produced natrolite-group minerals. The zeolite minerals might have crystallized at about 50–100 °C. Two generations of calcite and aragonite are the dominant carbonate minerals in the vesicles of the basalts. As the latest step, epigenetic minerals, such as Mn oxide minerals and goethite formed.

2. Field stops

2.1 Field stop 1: Tihany

Location: The village of Tihany (population ~1500) is situated on a peninsula on the northern shore of Lake Balaton, at the eastern side of the Bakony–Balaton Highland Volcanic Field. The whole peninsula is a historical district with the Benedictine Abbey in the centre (founded in 1055, rebuilt in 1754). The founding charter of the Abbey (the original is presently in the Pannonhalma Abbey, NW Hungary) is the first existing document containing Hungarian words, among them *ásvány*, the Hungarian term for "mineral" (in the charter used as a locality name; Papp, 2002).

Co-ordinates: N 46°54′50.80″ and E 17°53′14.79″; elevation: 100-200 m

Geology: The Tihany Maar Volcanic Complex (TMVC) represents the earliest (7.96 ± 0.03 Ma, Wijbrans *et al.*, 2007) volcanic products of post-extensional alkaline basaltic volcanism in the BBH. The remnant consists of several eruptive centres (western, central and eastern maars, Németh *et al.*, 1999) (Fig. 12). Initial base surge and fallout deposits were formed by phreatomagmatic explosions, caused by interaction between water-saturated sediments and rapidly ascending alkali basalt magma carrying dominantly peridotite xenoliths (Németh *et al.*, 2001). Subsequently, the deep excavated maar functioned as a local sediment trap where inflows of reworked or remobilized scoriaceous tephra built up Gilbert-type delta sequences (Németh *et al.*, 2001). The nature of the TMVC maar eruptions and their deposits appear to be strongly dependent on the hydrologic condition of the fracture-controlled aquifer, which varies seasonally because of its dependence upon rainfall and spring runoff (Németh *et al.*, 2001). The best preserved

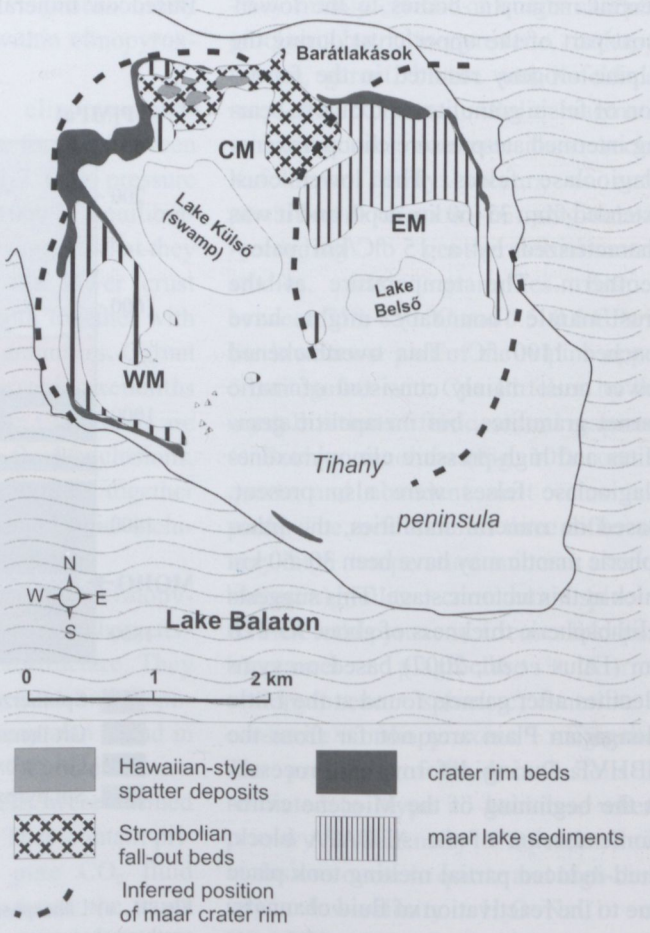

Fig. 12. Simplified geological map of the Tihany Peninsula showing the position of volcanosedimantary rocks, modified after Németh *et al.* (2001). Dashed line: inferred position of maar crater rim. Abbreviations: CM – Central Maar, EM – Eastern Maar, WM – Western Maar.

maar–crater rim sequence is located at the north-east side of the East Maar (Barátlakások). The hydrovolcanic activity was followed by Strombolian and minor Hawaiian magmatic explosive period, indicating a cut of water supply from the basement rocks.

Xenoliths: Peridotite xenoliths are hosted in well-exposed maar sediment, characterized by orthopyroxene-rich spinel lherzolites and spinel harzburgites, composed of only anhydrous silicates (olivine, orthopyroxene, clinopyroxene) and spinel (Fig. 13a). The average grain size of the peridotites studied here is coarser than that of the common peridotites of the BBHVF (max. 1–2 mm), because the fabric is dominated by 1–5 mm large orthopyroxenes and 2–4 mm sized olivines. In contrast, clinopyroxenes and spinels are generally smaller with their 40–300 μm and 20–100 μm size, respectively. Besides, the coarse-grained orthopyroxenes often enclose mostly euhedral or subhedral olivine as crystal inclusion (Figs. 13a–b). Furthermore, spinel can be present either as anhedral/subhedral crystal inclusion enclosed in the silicates (characteristic) or as an interstitial phase (Fig. 13a). Therefore, the dominant texture type of the peridotite xenoliths from Tihany was addressed as poikilitic (*e.g.* Embey-Isztin, 1984; Embey-Isztin *et al.*, 1989). Additionally, protogranular and equigranular textured xenoliths have also been described from here (Falus & Szabó, 2004). The crystallographic preferred orientation analysis of olivines suggests that the peridotite xenoliths were deformed even if their present texture shows no evidence for deformation (Falus & Szabó, 2004; Hidas, 2006). The supposed deformation process of the olivine is very similar to those of the peridotites of the BBHVF with deformed textures (Falus, 2004). Based on the orientation analysis, the deformation could be active before the development of the present poikilitic texture of the peridotites. The olivines (either as rock-forming mineral or as enclosed mineral inclusions) and pyroxenes can be characterized by high mg# (opx: 0.88–0.92; ol: 0.90–0.91, cpx: 0.88–0.93), whereas the Cr_2O_3 and Al_2O_3 concentration in the spinel ranges from 12.8 to 40.8 and 25.3 to 54.9, respectively. The geothermometric calculations based on the peridotites show a wide range of equilibrium temperature continuously between 925-1165 °C (±16 °C) which are more extended than that of peridotites collected from different outcrops in BBHVF. Based on the major element chemical composition, the petrographic observations and the international analogies, the origin of this poikilitic texture is thought to be the result of SiO_2-rich melt/wall rock interaction. Similar conclusion has been drawn by Bali *et al.* (2007) for the formation of orthopyroxene-rich mantle xenoliths from the same volcanic field but from different location (Szentbékkálla). High-density, negative crystal shaped fluid inclusions have also been found mainly in orthopyroxenes with unusually large amount (Figs. 13c–d), whereas inclusions in clinopyroxene are less common. By using the definition of Roedder (1984), this generation can be considered as either primary (single fluid inclusions) or pseudosecondary (appearing along healed fractures without reaching the mineral edges) fluid inclusions. Thus, the fluid inclusions might have been trapped from a fluid that interacted with the lithospheric mantle material. These fluid inclusions represent CO_2-rich (89–98 mol%), H_2S- (up to 1 mol%) and H_2O-bearing (2–11 mol%) fluid system as proved by Raman microspectroscopy at elevated temperatures (Berkesi *et al.*, 2009, Fig. 14). Trace elements, such as K, Ba, Rb, Nb and Ti were found to be linked to the fluid inclusions by in situ LAICP MS technique (Berkesi *et al.*, 2009; Szabó *et al.*, 2010). The results of fluid inclusion study suggest that the H_2O-bearing CO_2-rich fluids are important agents in the lithospheric upper mantle for transporting incompatible trace elements in the lithospheric mantle.

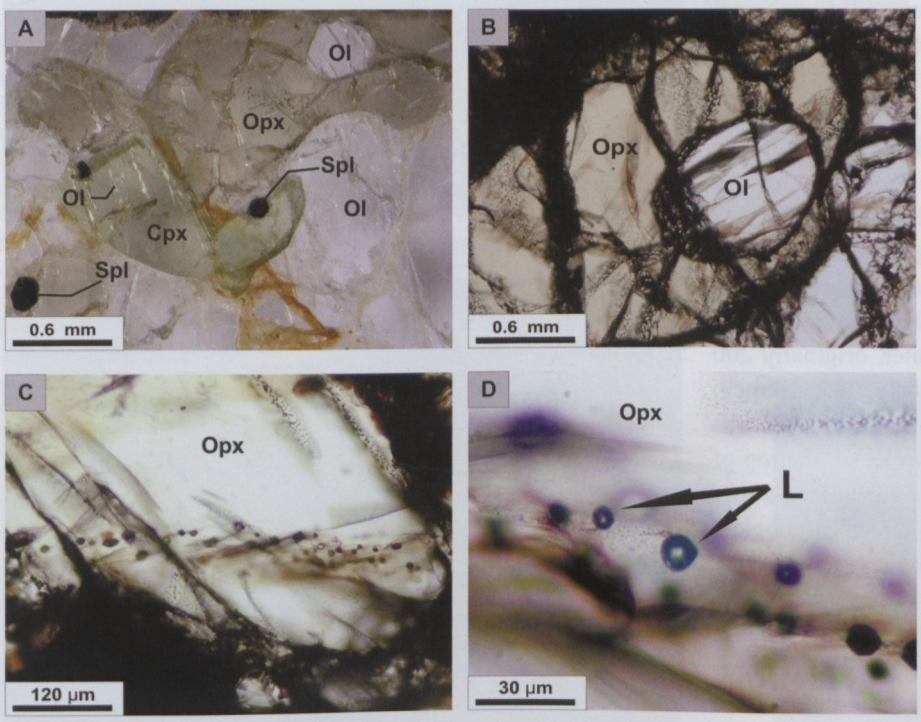

Fig. 13. Photomicrographs showing the petrographic characteristics of the Tihany peridotite series. A) The dominant orthopyroxene occurs together with clinopyroxene. Spinel can be mainly found as crystal inclusions, moreover, euhedral and subhedral olivines both in orthopyroxene and clinopyroxene have been found. B) Subhedral olivines as crystal inclusions hosted in orthopyroxenes. C) Orthopyroxene-hosted, negative crystal-shaped fluid inclusion trail. D) Partially decrepitated, negative crystal-shaped, at room temperature mainly one phase (liquid) fluid inclusions in a trail along healed fracture in orthopyroxene. Picture A: stereomicroscopic view, pictures B-D: plane polarized light, 1N. Abbreviations: Ol – olivine, Opx – orthopyroxene, Cpx – clinopyroxene, Spl – spinel, L – liquid.

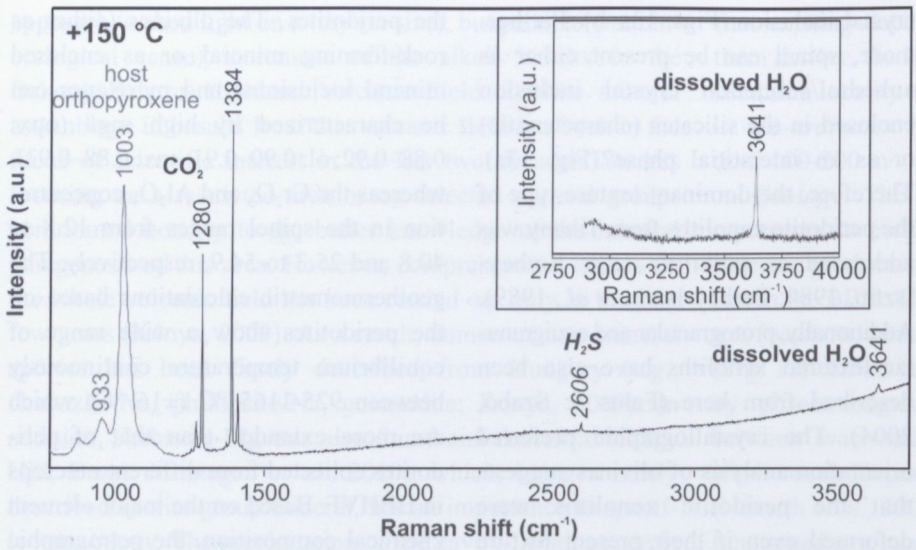

Fig. 14. Raman spectra with laser spot focused on individual phases in fluid inclusions at +150 °C: laser spot focused on the CO_2-rich phase; inset shows enlargement of the spectrum for dissolved water (peak position varies between 3638 and 3641 cm^{-1}). The presence of H_2S is probably related to the geological setting of the sub-continental lithospheric mantle (Berkesi *et al.*, 2009).

2.2 Field stop 2: Hegyes-tű Hill at Monoszló

Location: The Hegyes-tű Geological Exhibition Site (former basalt quarry) is situated near to the village of Monoszló, about 10 km north from the Lake Balaton, in the middle of the Bakony– Balaton Highland Volcanic Field.

Co-ordinates: N 46°54′48.24″ and E 17°38′4.46″; elevation: 300–350 m

Geology: The Hegyes-tű is a remnant of a coherent basanitic lava body, where no pyroclastic rocks have been found (Fig. 15). Ar/Ar dating shows that the lava is amongst the oldest volcanoes of the BBHVF with its 7.94 ± 0.03 Ma age (Fig. 4) (Wijbrans *et al.*, 2007). The locality is a 336 m high and about 200 m wide landmark in the Káli basin, formed by a columnar-jointed basanite plug. The 10–40 cm diameter columns are predominantly vertical, having some bends in the marginal zone of the exposure and convergent towards the top of the structure (Fig. 15). More than 220 m thick volcanic material was naturally eroded from the crater, originally 200 m in diameter, as calculated by 30 m/Ma erosion rate (Németh & Martin, 1999; Wijbrans *et al.*, 2007) and half of the hill was cut off by intensive quarrying in the past. Even so, the top of the hill is high enough to offer a spectacular view of a number of famous volcanoes in the BBHVF. Another volcanological curiosity, hyaloclastic volcaniclastic sediment (generated by magma-water interaction) occurs next to the main wall of the quarry (Fig. 16) (Németh & Martin, 1999; Martin & Németh, 2004). The alkaline basanite shows porphyritic microholocrystalline or trachytic texture and contain forsteritic olivine (Fo: 73–87) phenocrysts (0.2–3.0 mm in size) and minor Ti-rich augite microphenocrysts (up to 1 mm in size) in the groundmass (Ti-rich augite + labradoritic feldspar + Ti-magnetite + leucite + apatite) (Fig. 17). The olivine phenocrysts contain primary multiphase silicate melt inclusions (5-120 μm in size) consisting of glass + CO_2 (± CO) bubble + daughter minerals (rhönite + augite + apatite + Al-spinel + sulphide (pyrrhotite + chalcopyrite ± pentlandite) ± ilmenite ± rutile), CO_2 (± CO) fluid (2–15 μm in size) and trapped Cr-spinel inclusions (Kóthay *et al.*, 2005). Despite that trace element and isotopic compositions indicate the effects of an ear-

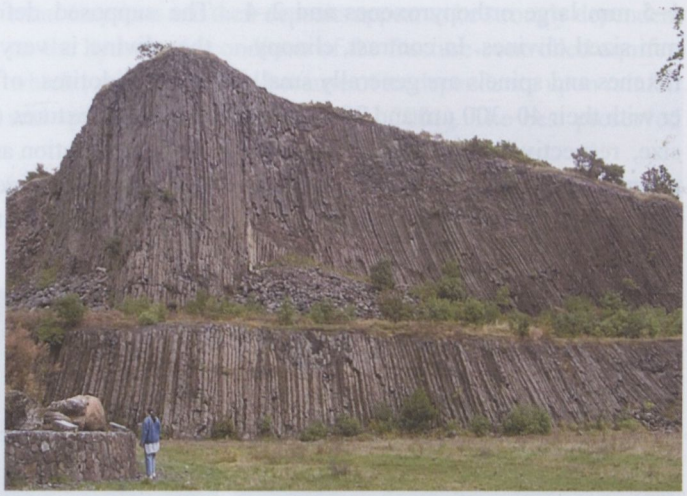

Fig. 15. Panoramic view of the columnar Hegyes-tű basanite cone.

Fig. 16. Hyaloclastite formation from the NE side of the Hegyes-tű quarry.

lier subduction, the source region of the basanitic magma is dominated by a lithospheric component and an asthenospheric origin (Embey-Isztin *et al.*, 1993). The magma can be characterized by high mg number (mg# [100*Mg/(Mg+Fe)] = 64.9 (Embey-Isztin *et al.*, 1993) and 61.7 (Kóthay, 2010)], low saturation index (S.I. = –23.4), differentiation index (D.I. = 33.3) and relatively high normative nepheline content (13.4%; Embey-Isztin *et al.*, 1993) of the bulk basaltic rocks. This indicates only a moderate degree of differentiation showing origin from a relatively primitive magma (Kóthay, 2010). The first phase to crystallize from the magma was the 82–87 mg# olivine phenocrysts (Fig. 17) containing Cr-rich spinel inclusions, primary CO_2-rich fluid, and primary silicate melt inclusions (SMI) (Fig. 18). According to the heating-freezing experiments, olivine phenocrysts may have started to crystallize at 1310–1260°C and minimum 0.7 GPa being in equilibrium with magma. SMI show more mafic character and are richer in alkalis: SiO_2 (40–46 wt%), Al_2O_3 (15–20 wt%), FeO (5–12 wt%), MgO (3–11 wt%), TiO_2 (2–3.5 wt%), CaO (10–15 wt%), Na_2O (3–6 wt%), K_2O (2–5 wt%) compared to that of the host rock and indicate a relatively oxidized environment (Kóthay *et al.*, 2005). Based on the geochemical study of the SMI, the evolution of the magma started with silicate – sulphide melt exsolution and immiscibility followed by sulphide bleb and then Al-spinel → rhönite → Ti-augite → apatite ± rutile ± ilmenite crystallization sequence (Kóthay *et al.*, 2005; Kóthay, 2010). The Si-rich residual magma has quenched into Na- and/or K-rich glass (Fig. 19). The silicate melt inclusions are richer in all trace elements compared to the host rock, which show the compositions of the silicate melt inclusions are more useful to show the geochemical differences of the melts than the bulk rock analyses (Fig. 20) (Kóthay, 2010). Based on the analysis of the reaction rim of middle crust quartz xenocrysts, these inclusions have been in the magma for 13 to 28 hours (Fig. 21) (Kovács *et al.*, 2003).

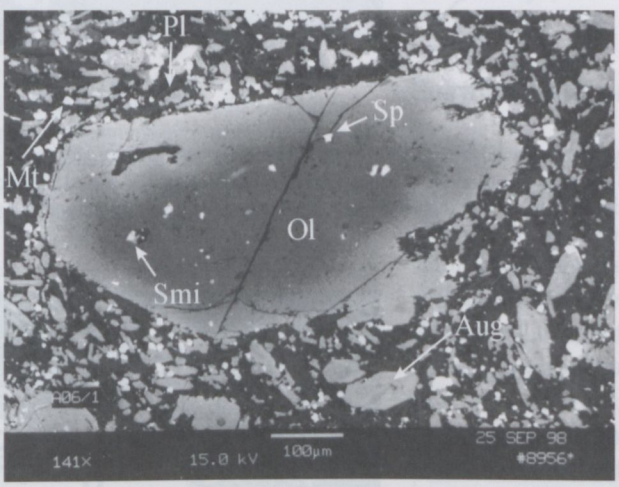

Fig. 17. BSE image of the porphyritic Hegyes-tű basanite containing zoned olivine phenocryst and clinopyroxene and plagioclase microphenocryst. The olivine phenocryst contains multiphase, partially crystallized, silicate melt inclusions (SMI) and spinel inclusions. Scale bar 0.1 mm. (Kóthay *et al.*, 2005)

2.3 Field stop 3: Szentbékkálla

Location: The village of Szentbékkálla (population ~250) is situated in the middle of the Bakony–Balaton Highland Volcanic Field, about 10 km north from the Lake Balaton.

Co-ordinates: N 46°53′26.30″ and E 17°33′52.66″; elevation: 150–200 m

Geology: Mapping of the area of Szentbékkálla village reveals small-volume pyroclastic flow deposits inferred to be a result of phreatomagmatic explosive eruptions, previously referred as hydroclastic flow deposits to describe their unusual textural characteristics (Németh *et al.*, 1999). The massive, unsorted, coarse-grained lapilli tuff beds alternate with cross-bedded, matrix-rich,

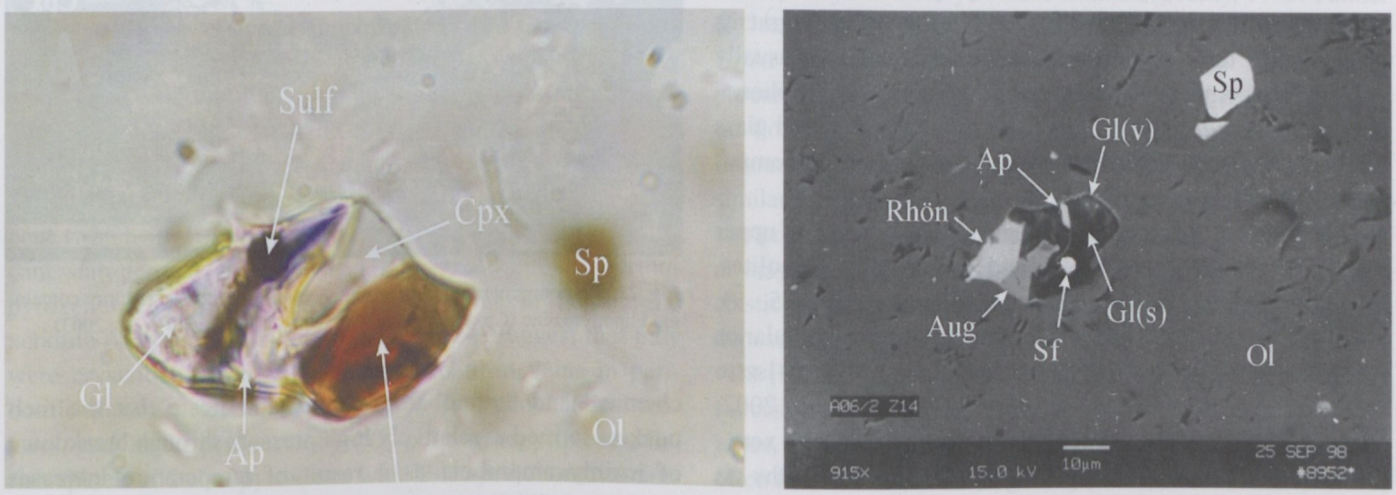

Fig. 18. Photomicrograph (1000x, 1N) (A) and BSE image (B) of partially crystallized multiphase silicate melt inclusions consisting of sulfide bleb (Sf/Sulf), rhönite (Rhön), augite (Aug), apatite (Ap), K-rich glass (Gl(v)) and Na-rich glass Gl(s) hosted in the core of an olivine phenocryst (Ol) from Hegyes-tű basanite. Spinel inclusion (Sp) is also shown.

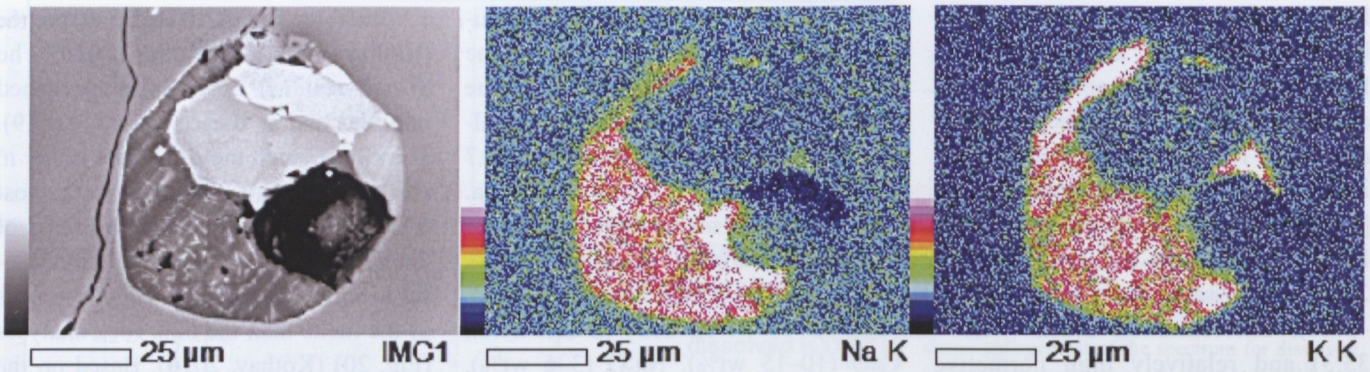

Fig. 19. BSE image and element map (Na and K) of partially crystallized multiphase silicate melt inclusion in olivine phenocryst from Hegyes-tű basanite.

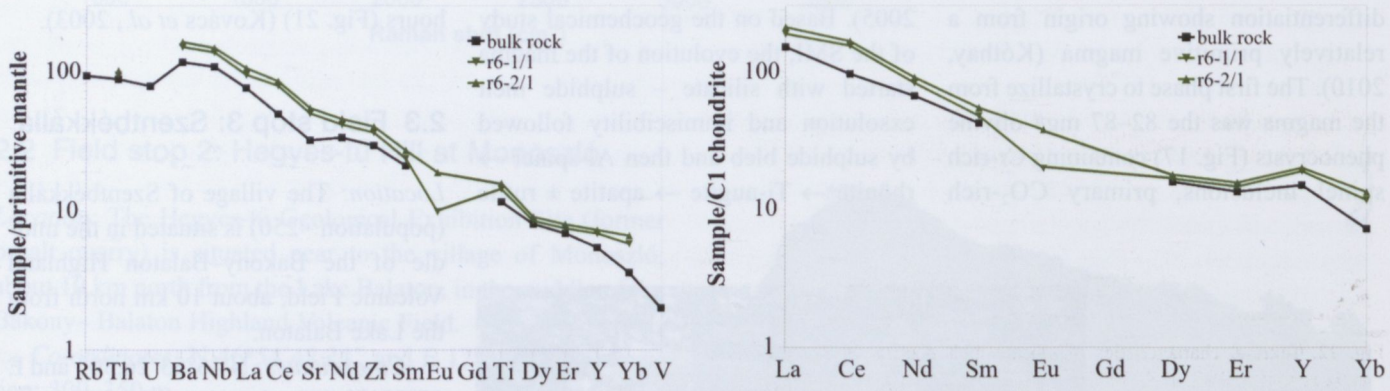

Fig. 20. Trace element composition of silicate melt inclusions (r6-1/1, r6-2/1) hosted in olivine phenocrysts from Hegyes-tű basanite compared to that of bulk rock of the host basanite. Multielement compositions are normalized to the primitive mantle (McDonough & Sun, 1995) and REE compositions are normalized to C1 chondrite (Nakamura, 1974). Green symbols refer to silicate melt inclusion (SMI) compositions, black symbol refers to bulk rock composition.

block-bearing lapilli tuff beds. The main body of the pyroclastic sequences consists of grey, massive, compact lapilli tuff beds. There is neither any evidence of grading or well-developed sedimentary structures nor welding in this unit. The lapilli tuff contains a high proportion of semi-rounded to rounded gravel-like ultramafic xenoliths, broken olivine and clinopyroxene xenocrysts without any systematic accumulation pattern (Martin & Németh, 2004). The juvenile fragments of the lapilli tuffs and tuffs from Szentbékkálla are usually ranging from tephrite through phono-tephrite to tephriphonolite (Németh *et al.*, 1999). Small, altered, light coloured glass shards show dacite/trachydacite and basaltic andesite composition (Németh *et al.*, 1999).

Xenoliths: at this locality (Fig. 4) a large amount of upper mantle peridotites, pyroxenites and sporadically granulites, calc-silicates and buchites have been found (Fig. 5, 9). Usually, the peridotites are coarse-grained and equigranular or porphyroclastic, rarely protogranular in texture (Embey-Isztin *et al.*, 1989; 2001; Downes *et al.*, 1992; Bali *et al.*, 2002; Falus, 2004; Szabó *et al.*, 2004). Some particular mantle xenoliths have also been found here. Mantle xenoliths at Szentbékkálla location frequently have melt pockets, which contain silicate minerals, glass, and often carbonate globules (Fig. 22) (Bali *et al.*, 2002, 2008b; Bali, 2004). Textural, geochemical and thermobarometric data indicate that the melt pockets formed at relatively high pressure through breakdown of mainly amphibole as a result of temperature increases accompanied, in most cases, by the influx of external metasomatic agents (Fig. 23). New trace elemental and Sr–Nd–Pb isotope data show that in several xenoliths the external agent

Fig. 21. Photomicrograph of quartz xenocryst (Q) with reaction rim containing clinopyroxene (Cpx) and glass (Gl). 200x, 1N (Kovács *et al.*, 2003).

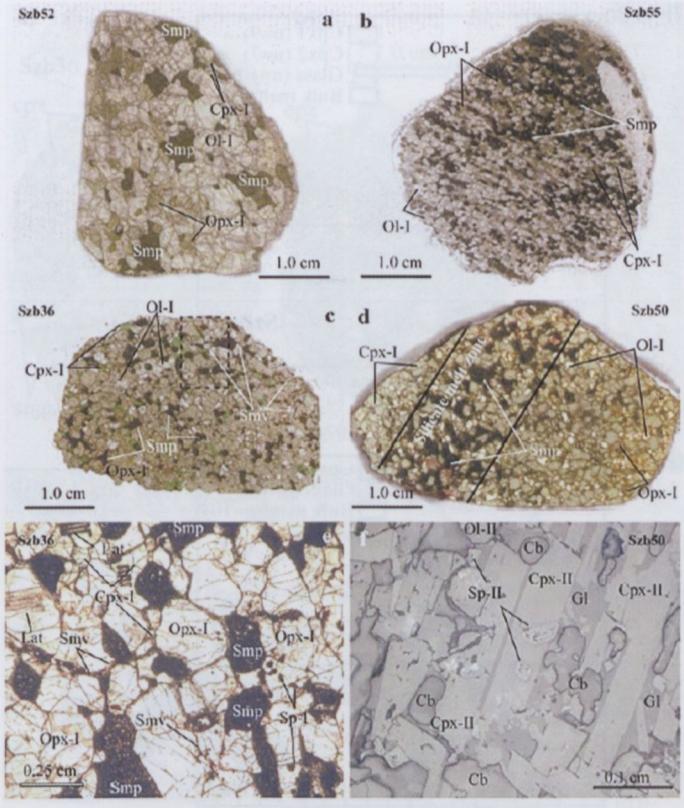

Fig. 22. Textural characteristics of silicate melt pockets in Szentbékkálla mantle xenoliths (Bali *et al.*, 2008b). a–d) Scanned thin sections. a) Irregular, isolated silicate melt pockets (Smp) in harzburgite Szb52. b) Elongated, interstitial melt pockets along the lineation of lherzolite Szb21. c) Melt pockets connected by silicate melt veins (Smv), forming irregular network in orthopyroxene-rich olivine websterite Szb36. d) Network-forming melt pockets concentrated in melt-rich zone of Szb50 olivine clinopyroxenite. e) Photomicrograph of network-forming melt pockets and veins in Szb36 (image location shown by dashed line in c) (plane polarized light). f) Microtexture of melt pockets with newly formed clinopyroxenes (Cpx-II), spinels (Sp-II), olivines (Ol-II), carbonate globules (Cb) and interstitial glass (Gl) in Szb50 olivine clinopyroxenite (reflected light). (Abbreviations: Ol-I – mantle olivine, Opx-I – mantle orthopyroxene, Cpx-I – mantle clinopyroxene, lat – laser ablation track).

was either a LIL-enriched aqueous fluid or a CO_2-rich fluid, whereas in other xenoliths the melt pockets were additionally enriched in LREE and sometimes HFSE, suggesting metasomatism by a silicate melt. The compositional character of the external agents might have been inherited by melting of a hydrated and probably carbonated deeper lithospheric component, which itself was metasomatized by melts with significant slab-derived components (Bali *et al.*, 2008b). Orthopyroxene-rich olivine websterites as veins in harzburgite xenolith or as individual xenoliths (Fig. 24) suggest that they were crystallized from silicate melts to form veins in peridotitic mantle rock (Bali *et al.*, 2007). Their geochemical features, such as the presence of Al_2O_3-poor orthopyroxenes, Cr-rich spinels and clinopyroxenes with U-shaped chondrite-normalized REE patterns (Fig. 25) indicate that the vein material formed from Mg-rich silicic (boninitic) melts at mantle depths (Bali *et al.*, 2007). The olivine fabric study of both the veins and the wall rock (Fig. 26) suggest that the development of the veins was followed by subsequent recrystallization during the Cenozoic evolution of the Carpathian-Pannonian region (Bali *et al.*, 2007). Peridotite xenoliths showing unusual tabular equigranular textures (addressed as flattened tabular equigranular) were also found here (Fig. 5). The olivines have a characteristic crystallographic preferred orientation (CPO) with [010] axes perpendicular to the foliation and the [100] and [001] axes forming a continuous girdle in the foliation plane (Hidas *et al.*, 2007) (Fig. 27). The deformation micro-mechanisms of olivines are suggested to be the activation of (010)[100] and also probably (010)[001] as the result of flattening during the complex tectonic evolution of the region (Hidas *et al.*, 2007). The lower crust is represented exclusively by mafic garnet granulites (Fig. 9). Even these garnet granulites are quite rare in this locality and most of them contain only pseudomorphs after garnet (Fig. 28) (Dégi *et al.*, 2010). Garnet granulite xenoliths in this locality are mostly composed of anhydrous minerals (Fig. 9). Amphibole was found very rarely. Abundant upper crustal limestones, sandstones, rhyolites, and rarely buchites, calc silicates are also found in this locality (Török *et al.*, 2005).

2.4 Field stop 4: Szigliget

Location: The village of Szigliget (population: ~900) is situated on the northern shore of the Lake Balaton at the western side of the Bakony–Balaton Highland Volcanic Field, 15 km southwest from the village of Szentbékkálla. Until 1822 the area was an island in the Lake Balaton. On the top of the hill of the town stand the ruins of a medieval fortress.

Co-ordinates: N 46°47′39.85″ and E 17°26′21.87″; elevation: 100–230 m

Geology: The village of Szigliget is situated on a small peninsula that used to be an island during high water stands of the 17,000 years history of Lake Balaton (Cserny, 1993; Tullner & Cserny, 2003). Volcanic products, dated to 4.53 ± 0.05 Ma by Ar/Ar technique (Wijbrans *et al.*, 2007), are the result of phreatomagmatic explosive activity, which generated pyroclastic flows (pyroclastic density currents) and phreatomagmatic fallout tephra. The volcanic rock beds in each hillside show similar north-westward dip direction and similar textural and compositional characteristics, suggestive of a complex, but closely related volcanic system in the area (Fig. 29). The pyroclastic rocks are interpreted as remnants of a former crater rim deposit around a maar basin that subsequently subsided into a vent (Németh *et al.*, 2000). At different levels of the volcanic successions, lower crustal buchites, mafic and metapelitic granulites, as well as upper mantle pyroxenites and peridotites are often found as xenoliths (Fig. 5, 9) (Török, 2002; Embey-Isztin, *et al.*, 1989; 2003; Downes *et al.*, 1992).

Xenoliths: Besides the common spinel peridotites, several special lithologies have been reported from here. Pargasitic

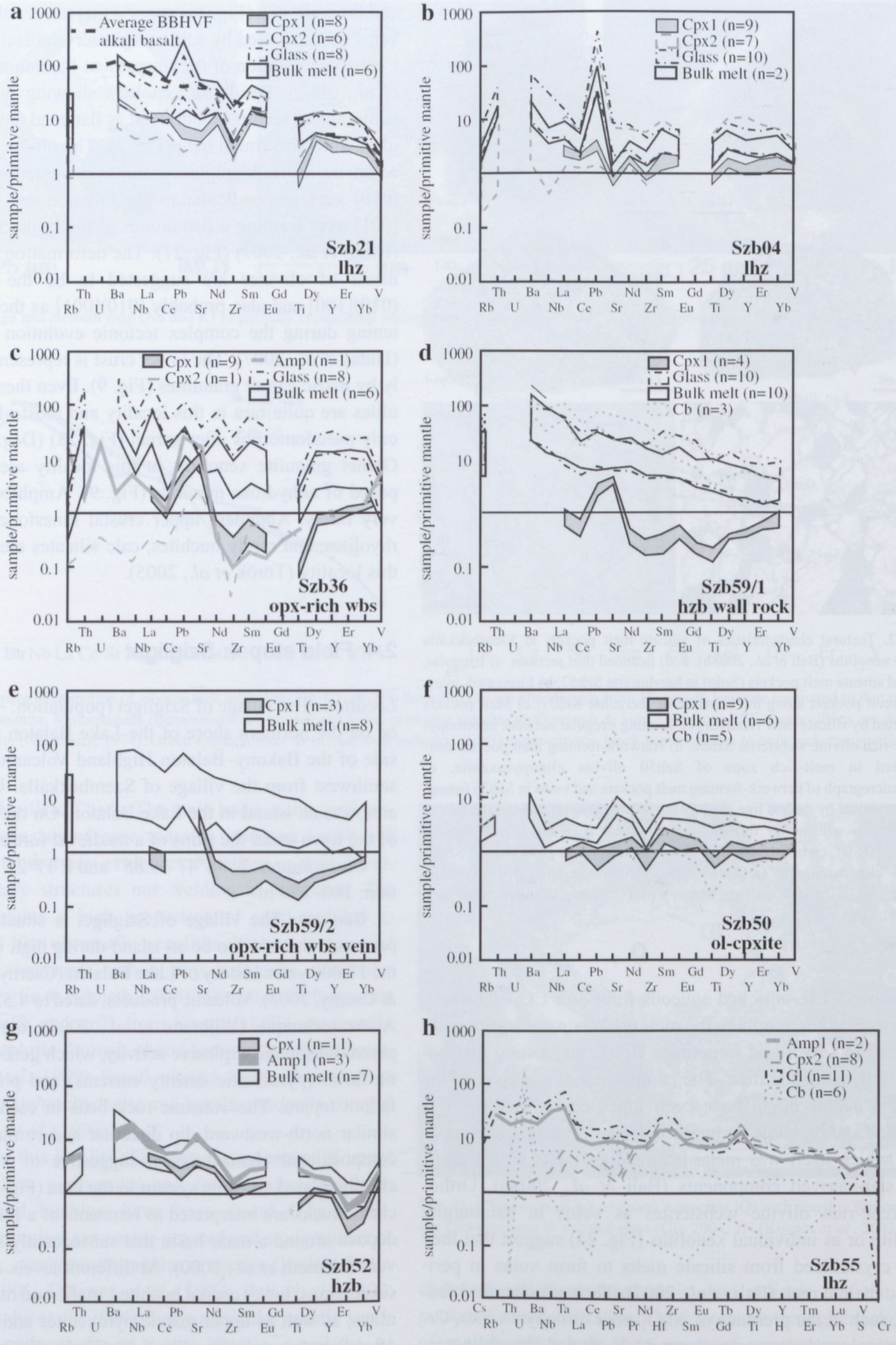

Fig. 23. Primitive mantle-normalized trace element patterns of primary amphiboles (Amp-I), primary clinopyroxenes (Cpx-I) and phases of silicate melt pockets (smp) (Bali *et al.*, 2008b). All analyzed glass (Gl) data are reported, whereas compositional ranges are shown for carbonate (Cb), newly formed clinopyroxenes (Cpx-II), bulk melt and mantle minerals. Normalizing values from McDonough & Sun (1995). n = number of analyses. An average BBHVF alkali basalt is shown in a) for comparison (Embey-Isztin *et al.*,1993; Harangi, 2001).

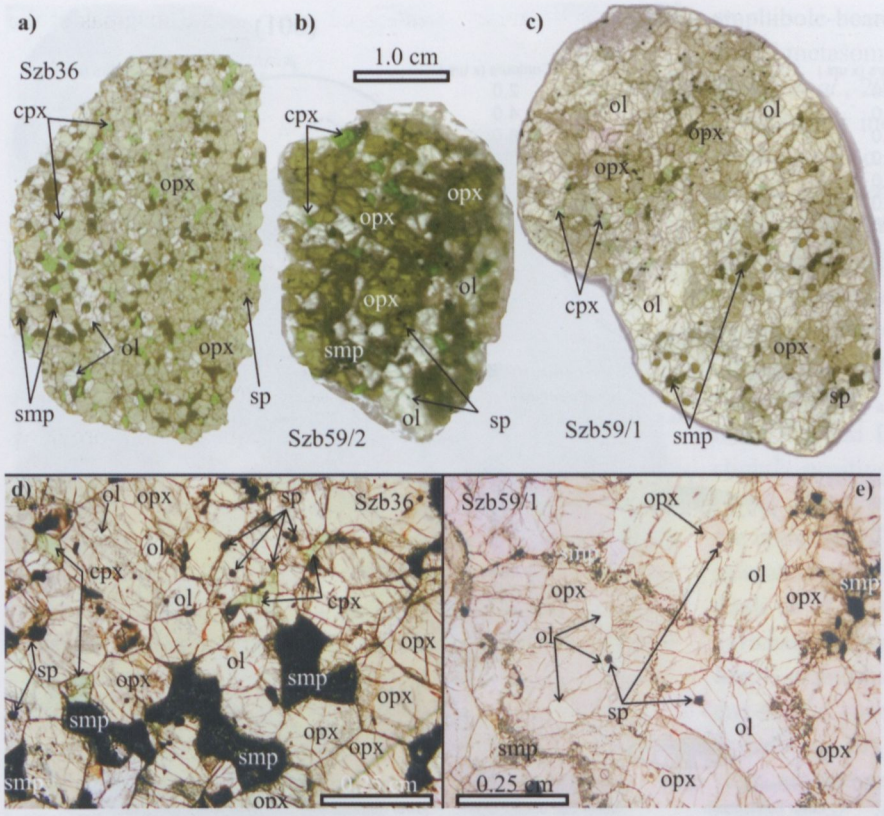

Fig. 24. Texture of orthopyroxene-rich olivine websterites Szb36 (a) and Szb59/2 (b) and harzburgite wall-rock Szb59/1 (c) (Bali *et al.*, 2007). a–c) Distribution of phases in the orthopyroxene-rich and harzburgite material of the studied xenoliths. Scanned thin sections. d) Photomicrograph of orthopyroxene-rich olivine websterite Szb36 with poikilitic texture, showing euhedral olivine inclusions in orthopyroxenes. Plane polarized light. E) Photomicrograph of harzburgite wall-rock Szb59/1 with poikilitic texture, showing euhedral olivine inclusions in orthopyroxenes and orthopyroxene inclusions in olivines. Plane polarized light. (Abbreviations: ol – olivine, opx – orthopyroxene, cpx – clinopyroxene, sp – spinel, smp – silicate melt pocket).

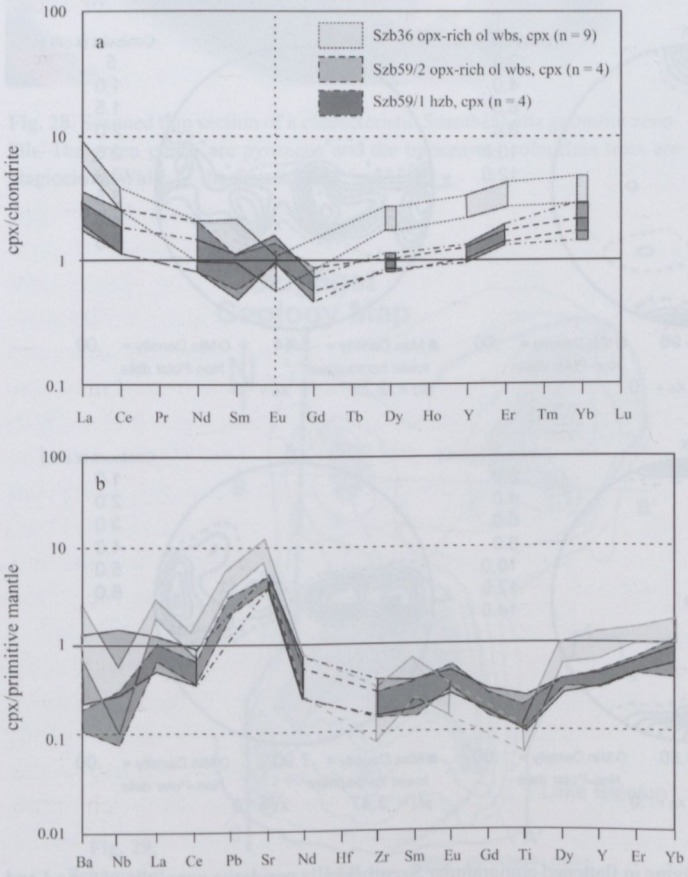

Fig. 25. Chondrite-normalized rare earth element (a) and primitive mantle-normalized trace element (b) diagrams for clinopyroxenes in orthopyroxene-rich olivine websterites (Szb63 and Szb59/2) and harzburgite wall-rock (Szb59/1). Normalizing values are from Anders & Grevesse (1989) and McDounough & Sun (1995), respectively (Bali *et al.*, 2007).

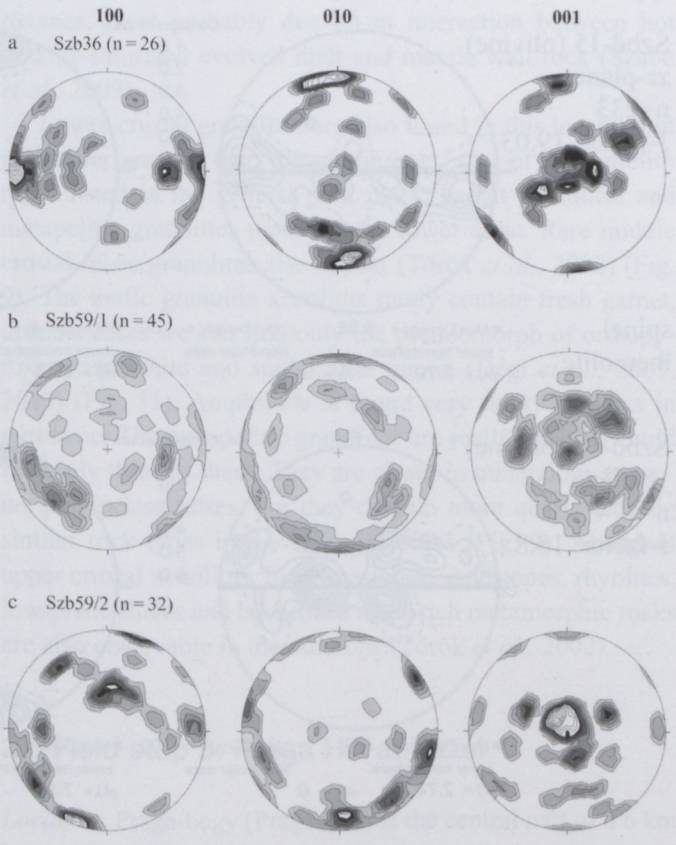

Fig. 26. Stereograms of olivine orientations in the Szentbékkálla peridotite xenoliths of orthopyroxene-rich olivine websterites (Szb63 and Szb59/2) and harzburgite wall-rock (Szb59/1). All axes exhibit low distribution maxima. Lower hemisphere, equal area projection. Data contoured at 1, 2, 3,. . . times uniform distribution. n – Number of measured grains (Bali *et al.*, 2007).

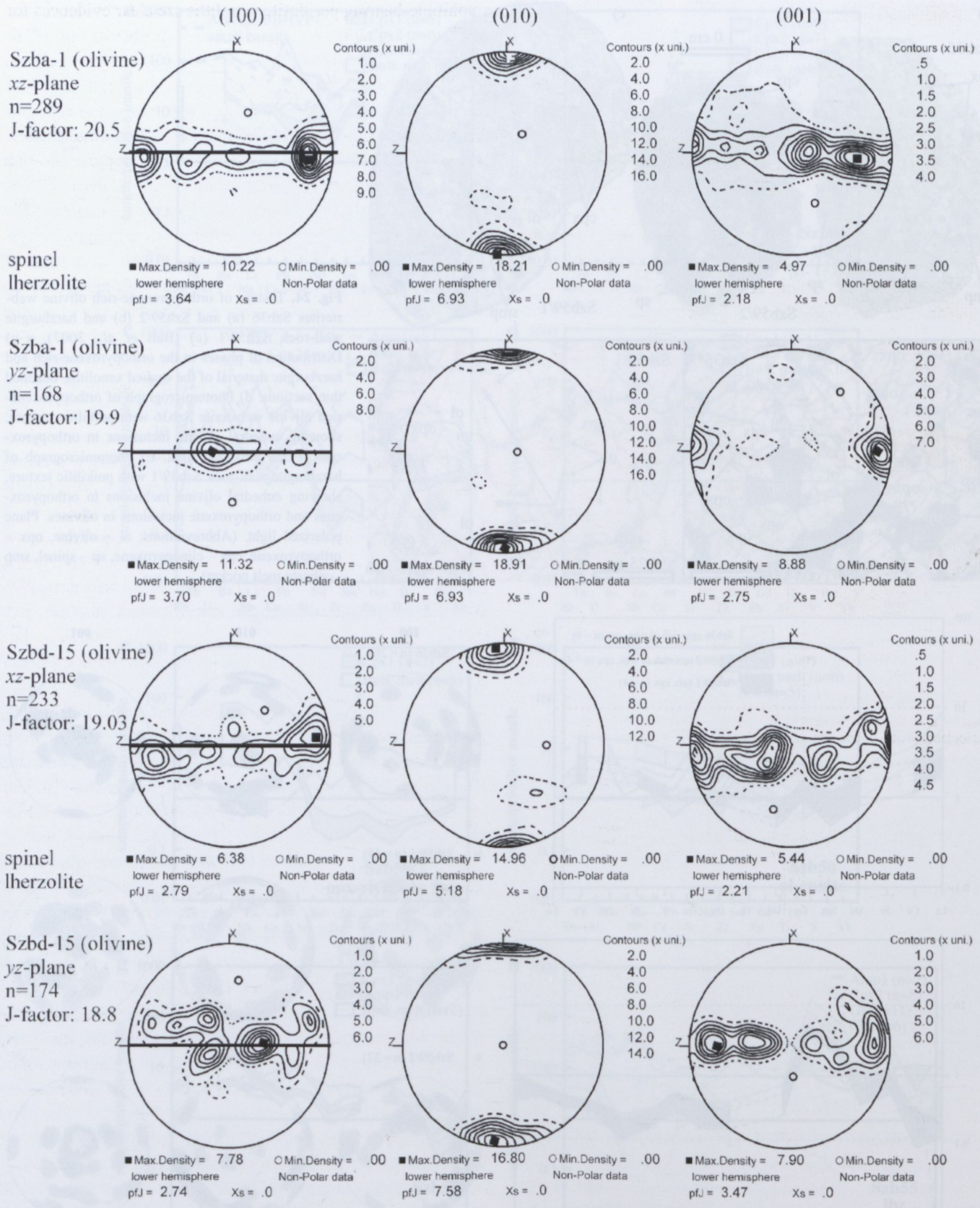

Fig. 27. Crystallographic preferred orientation (CPO) patterns and *J* factor of olivine in flattened equigranular Szentbékkálla peridotite xenoliths of Szba-I and Szbd-15. Pole figures are lower hemisphere, equal area projections, using PF2k (Mainprice, 2003). Horizontal lines denote the foliation, lineation at 90°/0°. Sectioning inaccuracies were corrected, by rotating the data (Hidas *et al.*, 2007).

Fig. 28. Scanned thin section of a characteristic Szentbékkálla granulite xenolith. The green grains are pyroxene and the transparent colourless ones are plagioclase. Width of the xenolith is 4.5cm.

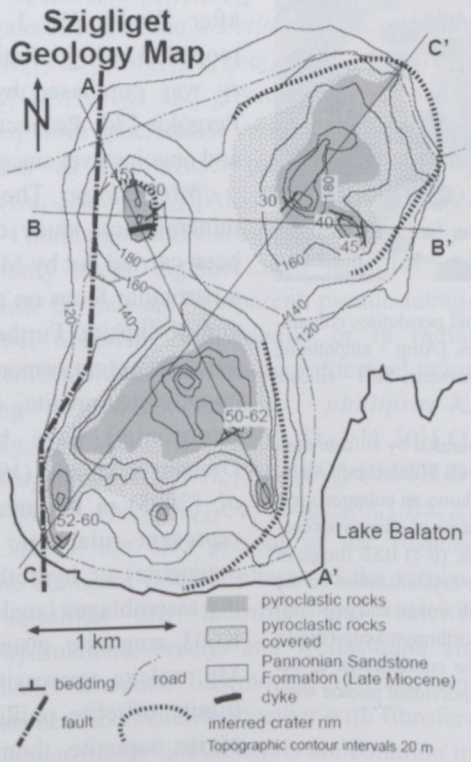

Fig. 29. Schematic overview of the Szigliget maar/diatreme (after Németh *et al.*, 2000).

amphibole-bearing peridotite xenoliths are clear evidences for modal metasomatism beneath the region (Embey-Isztin, 1976; Szabó *et al.*, 2009). Similarly, in several peridotites, isolated silicate melt inclusions or coexisting silicate melt and fluid inclusions also indicate percolation of metasomatic melts in the subcontinental lithospheric mantle (Szabó *et al.*, 2009; Hidas *et al.*, 2010). In a quartz-bearing orthopyroxene-rich websterite xenolith, both ortho- and clinopyroxenes contain primary and secondary silicate melt inclusions, and rounded or needle-shaped quartz occurs as inclusions in orthopyroxene (Bali *et al.*, 2008a). The melt inclusions are SiO_2- and alkali-rich and MgO-, FeO-, CaO-poor. They are strongly enriched in LREE and LILE and display negative Nb-, Ta-, Sr- and slightly positive Pb-anomalies. The xenolith is interpreted to be a fragment of an orthopyroxene-rich body, which formed in the upper mantle by interaction of mantle peridotite with a Si-saturated silicate melt released from a subducted oceanic slab (Bali *et al.*, 2008a). Evidence for the percolation of silica-enriched melts has been also found in amphibole-bearing peridotite xenoliths containing clinopyroxene- and orthopyroxene-hosted coexisting silicate melt and carbonic fluid inclusions (Fig. 30). The coexisting silicate melt and fluid inclusions are the result of immiscibility at mantle PT conditions (Hidas *et al.*, 2010). The entrapment of inclusions happened after partial melting and subsequent crystallization of clinopyroxenes, most probably due to an interaction between hot volatile-saturated evolved melt and mantle wall-rock (Szabó *et al.*, 2009).

Lower crustal granulites are also found in this locality but in smaller amount than ultramafic ones. Out of the xenolith types listed in the general part, mafic garnet granulites and metapelitic granulites represent the lower crust. Rare middle crustal felsic granulites also appear (Török *et al.*, 2002) (Fig. 9). The mafic granulite xenoliths rarely contain fresh garnet, in most cases we can find only the pseudomorph of orthopyroxene, anorthite and spinel after garnet (Dégi *et al.*, 2009, 2010) (Fig. 31). Amphibole is found very rarely as relics in pyroxene. The metapelitic granulites are really rare; we could find only three of them. They are closer in mineralogy to garnet-plagioclase felses, but they contain more quartz than do similar rock types in the other localities (Fig. 9). Abundant upper crustal xenoliths, like limestones, sandstones, rhyolites, low-grade shales and buchitized mica-rich metamorphic rocks are also observable in the outcrops (Török *et al.*, 2002).

2.5 Field stop 5: Prága Hill at Bazsi

Location: Prága-hegy (Prága Hill) is the central part of a 6 km long, NE–SW strike basalt ridge between the villages of Tátika and Sarvaly, at the western side of the Bakony–Balaton Highland Volcanic Field.

Co-ordinates: N 46°55′39.86″ and E 17°14′44.85″; elevation: 350 m

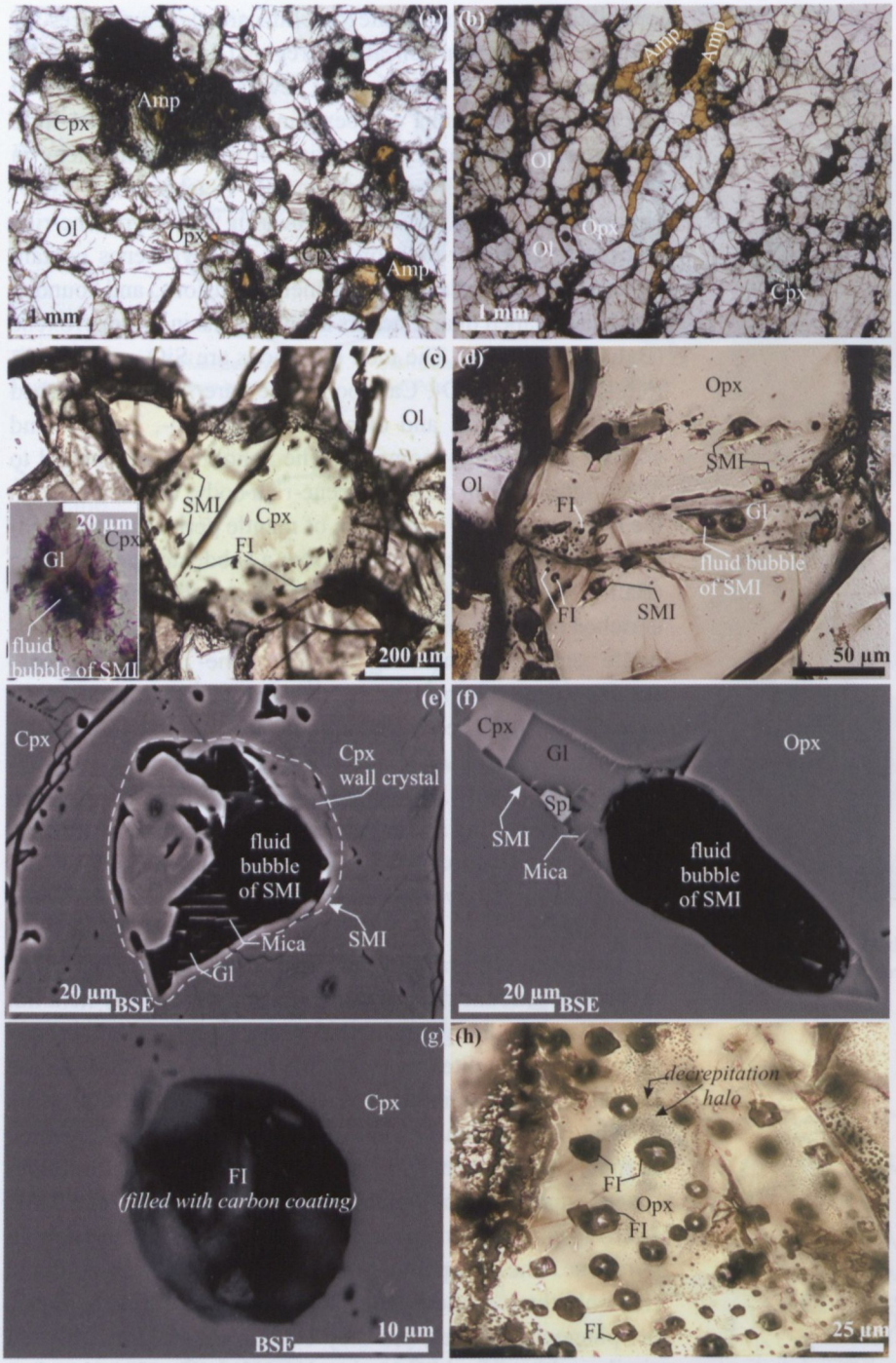

Fig. 30. Photomicrographs (1N, plane polarized light) of amphibole-bearing spinel peridotites containing coexisting silicate melt inclusions and fluid inclusions entrapped in pyroxenes. (Amp – amphibole; Cpx – clinopyroxene; FI – fluid inclusion; Gl – glass; Ol – olivine; Opx – orthopyroxene; SMI – silicate melt inclusion; Spl – spinel.)

(a) Equigranular texture of a spinel lherzolite with disseminated amphiboles surrounded by silicate melt pockets. (b) Equigranular texture of a spinel lherzolite with veined amphiboles. (c–d) Silicate melt inclusions and fluid inclusions in clinopyroxene (left) and orthopyroxene (right). Inset shows an enlarged view of a silicate melt inclusion entrapped in clinopyroxene. Note the differences in shape of clinopyroxene-hosted (irregular) and orthopyroxene-hosted (drop-shaped) silicate melt inclusions. (e–f) BSE image of silicate melt inclusion in clinopyroxene (left) and orthopyroxene (right). Note the crystallization on the wall of clinopyroxene-hosted inclusions resulted in their irregular shape. (g–h) BSE image and photomicrograph of negative crystal-shaped fluid inclusions in clinopyroxene (left) and orthopyroxene (right), respectively. The photomicrograph is a completely focused image created by the combination of the focused areas of several partially focused images using Helicon Focus software. Individual photos were taken at plane polarized light, 1N (Hidas *et al.*, 2010).

Geology: Prága Hill is part of the Tátika sill/dyke complex. Its volcanic rocks form finger-like units intruded to Upper Miocene – Pliocene lacustrine and alluvial sediments (Fig. 32). These dykes are irregular in shape, furthermore their show alteration in their few dm to 1 m thick rim zones caused by the surrounding rocks (Martin & Németh, 2004). The basaltic rocks and the overlying sedimentary layers are outcropped at the Karikás-tető quarry. These sedimentary rocks consist mostly of sandstones and claystones with minor fossil content. The dyke swarm was later outcropped due to still ongoing erosion of the topping Pannonian sedimentary formations.

Sedimentary rock fragments originating from the overlying layers or the underlying Neogene sediments can be found in the volcanic formation. Their composition is diverse as they include clay, sand and limestone and some quartz pebbles. Sedimentary rocks adjacent to the subvolcanic bodies have been affected by hydrothermal processes (Bodorkós, 1997; Martin & Németh, 2004).

The quarry at Bazsi was first mentioned in the scientific literature by Schafarzik (1904). Stone production has been significant until 1918 and declined after World War I. The quarry was reopened in 1959. In the 1990s the quarry was purchased by Austrian-owned Pergőkő Ltd. Production is continuous and ongoing ever since (Bodorkós, 2007).

Mineralogy: The first substantial mineralogical study on the quarry has been carried out by Mauritz (1948) with a particular focus on analcime, natrolite and phillipsite. Further minerals of the paragenesis (*e.g.*, saponite, okenite, pyrite, apophyllite, apatite, aragonite, calcite, thomsonite) have been studied by Drabant & Mozgai (1989) and Szakáll *et al.* (2005) in the area. These minerals represent miarolitic (apatite, augite, magnetite) or hydrothermal cavity-filling assemblages (analcime, apophyllite-KOH, aragonite, gismondite, chabazite-Mg, calcite, marcasite, natrolite, nontronite, offretite, phillipsite-Ca, -K, -Na, pyrite, saponite, thomsonite-Ca) in the

basalt or are related to altered xenoliths of sedimentary rocks (brucite, diopside, fibroferrite, hidromagnesite, hydrotalcite, quartz, lizardite, scawtite, wollastonite, tobermorite-11Å) in the basalt (Kovács-Pálffy *et al.*, 2007; Kónya, 2009). *Analcime* is found as light green crystals, 1 to 3 mm in diamater, they are mostly the {211} deltoid icositetrahedron combined with the faces of the cube {100}. *Gismondite*, $CaAl_2Si_2O_8 \cdot 4H_2O$, a rather rare zeolite in this locality, mostly occurs together with analcime. White, needle-like *natrolite*, $(Na_2[Al_2Si_3O_{10}] \cdot 2H_2O$, forms spherical aggregates (Fig. 33) 1 mm in diameter on the wall of vesicular cavities (Kovács-Pálffy *et al.*, 2007). Two generations of *calcite* can be found in the cavities. The first generation is characterized by rhombohedra, which occur individually (2-5 mm crystals) or are grouped in 1-2 cm large spherical aggregates (Fig. 34); these are commonly found together with phillipsite and chabazite. The second generation of calcite form mostly 4 to 7 mm large scalenohedral crystals occurring together with natrolite-group minerals. Two generations of *aragonite* can also be identified: 1) the first generation builds transparent, thin, elongated aggregates not exceeding 7 mm in size; 2) the second generation forms thicker, long prismatic crystals up to 20 mm but usually 4-5 mm in length (Fig. 35). *Chabazite* occur as transparent, 5 mm large, pseudorhomboedral crystals. Most of them have remarkably high Ca content. A new chabazite species has been identified from the outcrop using WDS by Montagna *et al.* (2010): *chabazite-Mg*, $(Mg_{0.67}K_{0.52}Ca_{0.48}Na_{0.08}Sr_{0.03})[Al_{3.16}Si_{8.89}O_{24}] \cdot 9.51H_2O$. *Apophyllite-KOH*, $(K_{0.87}Na_{0.05})Ca_{3.86}(Al_{0.05}Si_{7.79})O_{20}[(OH)_{0.99}F_{0.01}] \cdot 9.66H_2O$, occurs as transparent bipyramidal or pseudo-hexahedral, 3 to 5 mm large crystals. Transparent, less than 1 mm, hexagonal prismatic crystals of *offretite*, $(Mg_{1.17}Ca_{0.97}K_{0.92}Na_{0.04}Fe_{0.01}Sr_{0.01})[Al_{4.88}Si_{13.03}O_{36}] \cdot 7.59H_2O$, form radial aggregates. Most of the *smectites* have a saponitic composition $(Ca_{0.33}K_{0.13}Na_{0.11})(Mg_{3.82}Fe^{3+}_{0.76}Fe^{2+}_{0.47}Al^{VI}_{0.37}Mn_{0.01}Ti_{0.01})(Si_{6.96}Al^{IV}_{1.04})O_{20}(OH)_4 \cdot 9.12H_2O$ and green, brown or bluish grey in colour. They form spherical or vermicular aggregates (Fig. 36) or occur as fine crusts on older minerals. *Thomsonite-Ca*, $(Ca_{1.70}Na_{1.21}Sr_{0.08})[Al_{4.75}Si_{5.24}O_{20}] \cdot 6.15H_2O$, forms transparent, 4 mm large spherical aggregates on phillipsite. They commonly occur together with natrolite and gonnardite. *Phillipsite* crystals are transparent, pseudo-tetragonal and prismatic, occurring individually or in radial aggregates and often exhibiting the Marburg or Stempel twins forms. According to WDS analysis, *phillipsite-K*, $(K_{1.90}Ca_{1.84}Na_{0.19}Mg_{0.01}Fe_{0.01}Ba_{0.01})[Al_{6.09}Si_{9.98}O_{32}] \cdot 11.30H_2O$, *phillipsite-Ca*, $(Ca_{2.84}Na_{0.53}K_{0.21})[Al_{6.22}Si_{9.73}O_{32}] \cdot 10.95H_2O$, and *phillipsite-Na*, $(Na_{2.09}K_{1.62}Ca_{1.38}Mg_{0.01}Sr_{0.01}Ba_{0.01})[Al_{6.45}Si_{9.53}O_{32}] \cdot 11.31H_2O$, are also present in the vesicles (Kónya, 2009). The dominant mineral phases of the serpentine-containing xenoliths are lizardite and calcite. Hydromagnesite, hydrotalcite, brucite and wollastonite are also present in smaller amounts. Tobemorite-11Å has been identified in vesicles near the xenolith together with fibroferrite or scawtite. Hydrogrossular-like minerals are common in

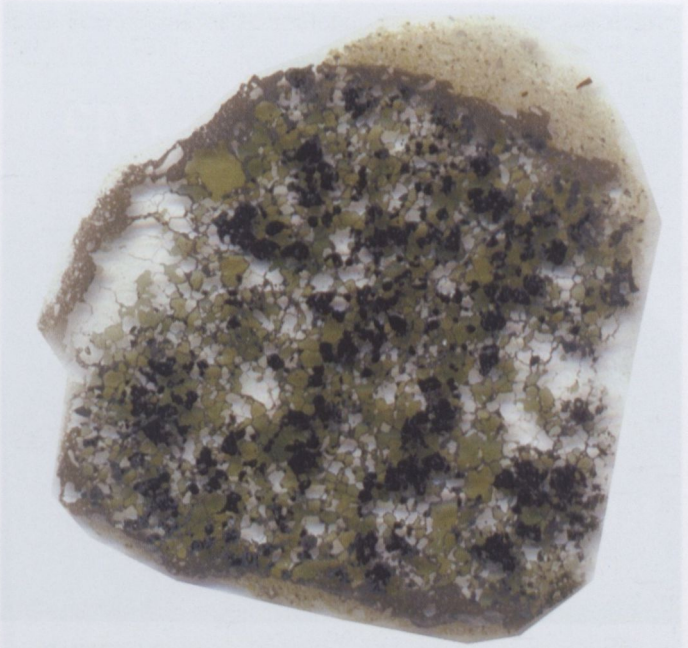

Fig. 31. Scanned thin section of a mafic garnet granulite xenolith from Szigliget. Note the black opaque-looking very fine-grained pseudomorphs after garnet. The green grains are pyroxene and the transparent colourless ones are plagioclase. Width of the xenolith is 4.5 cm.

Fig. 32. Overview of the sill of Prága Hill, Bazsi.

Fig. 33. Radial aggregates of natrolite needles, Prága Hill, Bazsi; image width 2.5 cm.

Fig. 34. Colourless, globular calcite crystal aggregates, Prága Hill, Bazsi; image width 1.2 cm.

Fig. 35. Aragonite (generation II) covered by green saponite, Prága Hill, Bazsi; image width 2 cm.

Fig. 36. Vermicular saponite, Prága Hill, Bazsi; image width 1 cm.

the contact zones (Kovács-Pálffy *et al.*, 2007; Kónya, 2009). Besides serpentine xenoliths, quartz inclusions can also be found. These mostly consist of fine- to coarse-grained quartz in the core and diopsidic and acmitic clinopyroxenes in the reaction rims.

2.6 Field stop 6: Haláp Hill at Zalahaláp

Location: Haláp Hill is found in the northern part of the Tapolca Basin. The former basalt quarry is located about 5 km north of the town of Tapolca. The quarry is abandoned.

Co-ordinates: N 46°55′26.45″ and E 17°27′26.37″; elevation: 331 m.

Geology: Haláp Hill is an erosional remnant of a maar/tuff ring volcano. The first phase of volcanism was characterized by phreatomagmatic explosions due to magma/water interaction followed by effusion of basaltic lava forming a lava lake in the crater and covering the pyroclastic ring (Németh & Martin, 1999; Martin & Németh, 2004). The basaltic rocks are vertically jointed with 4-6 dm wide hexagonal and pentagonal columns, which may reach heights up to 20 m (Fig. 37). The edge of the crater consists of sideromelane containing lapilli tuff and exhibiting a 1 m thick peperitic zone at its contact with the lava rocks (Németh & Martin, 1999; Martin & Németh, 2004). This zone indicates that basanitic lava intruded to a water-saturated non-consolidated tephra layer. The basaltic rocks intersect Mesozoic and overlaying Lower to Middle Miocene carbonates, and contacts Upper Miocene Pannonian sands on the surface. Contacted formations were sampled by the lava as it is supported by the presence of xenoliths in the lava rocks and of lithic clasts (~25 vol%) in the pyroclastite of the tuff ring (Martin & Németh, 2004). The age of coherent basanite lava has been determined by $^{39}Ar/^{40}Ar$ method indicating that the formation is 3.06 ± 0.02 My old (Fig. 4) (Wijbrans *et al.*, 2007). According to the calculations of Martin & Németh (2004) up to 208 m thick volcanic material has been eroded from the 1000 m diameter crater. The basalt mining was started in small quarries in 1909. Large-scale production began after World War I. Mining activity further developed and increased after World War II; in the 1950s the rock was extracted on three levels in nine quarries (Jugovics, 1955). The quarries were closed in the second half of the 1980s.

Basalt: The dominant phenocrystalline phase of the basalt is olivine, however clinopyroxenes also occur. The groundmass consists of plagioclase, clinopyroxene, magnetite, ilmenite and K-feldspar. Jugovics (1959) reported two textural types of basalt correlating with the colour of the rock. Darker basalts are characterized by thin, elongated plagioclase and small magnetite crystals. In the lighter basalts the proportion of K-feldspars is close to that of clinopyroxenes and their appearance is tabular or columnar. Magnetites are also larger in this type of rock. Embey-Isztin *et al.* (1993) distinguished two varieties, one with higher SiO_2 and another with higher MgO content. According to their results, Haláp basalts are relatively less unsaturated (mg# =

Fig. 37. Columnar basalt at Haláp Hill, Zalahaláp.

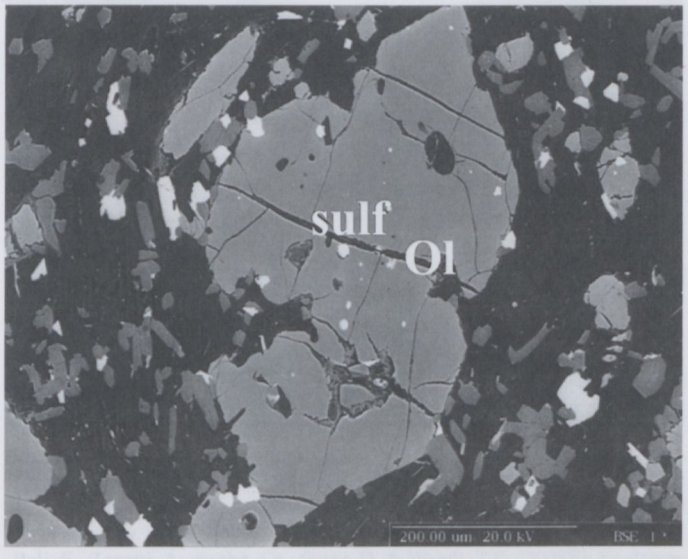

Fig. 38. BSE image of porphyritic Haláp basalt with zoned olivine (Ol) phenocryst containing large number of sulfide inclusions (sulf). Scale bar 0.2 mm.

[100*Mg/(Mg+Fe)]) 60.4–65.7; normative nepheline content: 0–3.35%; normative hyperstene content 0–1.35) than other alkali basalts of the CPR. Besides sulfide, spinel and orthopyroxene inclusions (Fig. 38), the 76–85 mg# olivine phenocrysts often also contain primary, coexistent silicate melt and fluid inclusions (Fig. 39). The composition of these silicate melt inclusions indicates a complex, heterogeneous melt system. Based on the geochemical study of the silicate melt inclusions, crystallization order was Al-spinel + sulfide → rhönite + amphibole + clinopyroxene → apatite ± ilmenite. The Si-rich residual melt has quenched into Na- and/or K-rich glass with significant amount of CO_2 (± CO ± CH_4) exsolved and trapped in the form of bubbles. Trace element composition of the silicate melt inclusions shows slight HREE depletion and no Sr peak compared to that of the bulk rock (Fig. 40).

Minerals: Fractures and cavities of the basaltic rocks contain a variety of mostly hydrothermal minerals (*e.g.*, Erdélyi, 1941; Mauritz, 1937, 1958; Váczi, 2003; Kónya, 2006, 2008).

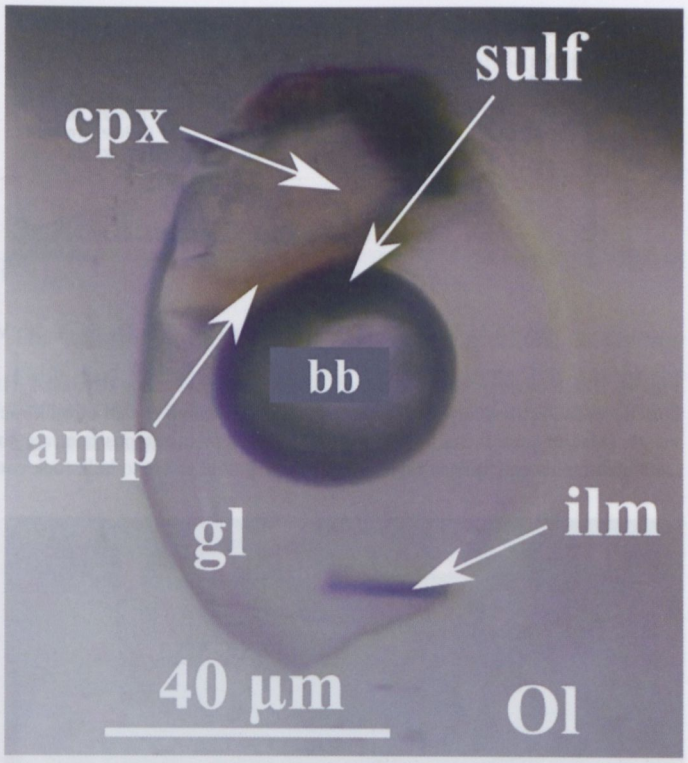

Fig. 39. Photomicrograph of primary, partially crystallized silicate melt inclusion hosted in olivine (Ol) phenocryst from Haláp basalt. Multiphase silicate melt inclusion consist of sulfide bleb (sulf), clinopyroxene (cpx), amphibole (amp), ilmenite (ilm), glass (gl) and CO_2-rich bubble (bb) (1N).

Zeolites (gismondine, natrolite, phillipsite) and calcite have been first described by Mauritz (1939) based on optical studies. Some mineral phases (*e.g.* analcime and apophyllite), new for the locality, were reported by Szakáll *et al.* (2005) without detailed investigations. Cavities of basalt contain miarolitic minerals (apatite, augite, magnetite, plagioclase and sanidine), zeolites (analcime, chabazite-Ca, chabazite-Na, garronite, gismondine, gmelinite-Ca, gmelinite-Na, gobbinsite, gonnardite-Na, natrolite, mesolite, phillipsite-Ca, phillipsite-K and phillipsite-Na) and other, secondary minerals (calcite, smectite, goethite and Mn oxides) (Kónya, 2009). *Apatite* forms colourless, transparent hexagonal crystals up to 1-3 mm. Based on the EDS analyses, apatite is *fluorapatite*. *Augite*, $(Ca_{0.78-0.81}Fe^{2+}_{0.18-0.24})(Mg_{0.75-0.79}Ti_{0.08-0.10}Fe^{2+}_{0.06-0.15}Fe^{3+}_{0.06}Al^{VI}_{0.03})(Si_{1.79-1.88}Al^{IV}_{0.12-0.21})O_6$, is the most frequent miarolitic mineral in the cavities. It forms brown to black, short prismatic crystals. *Magnetite* is found as black, idiomorphic octahedral crystals up to 0.5–1 mm, rarely 2–3 mm. According to the chemical analyses, magnetite always has a significant TiO_2 content (2.75–3.42 wt%) (titanian magnetite). *Plagioclase* occurs as colourless, thin tabular crystals (up to 3–6 mm). Based on EDS analyses, plagioclase is labradorite ($Ab_{25-89}An_{11-75}Or_{0-8}$). *Sanidine* forms colourless to white, small (~1 mm) tabular crystals. *Analcime*, $Na_{0.97}Ca_{0.01}[Al_{0.97}Si_{2.03}O_6]\cdot 1.02H_2O$, is a very rare mineral at the locality and it occurs as glassy, colourless deltoid icositetrahedral {211} crystals (3 mm). *Chabazite* forms glassy,

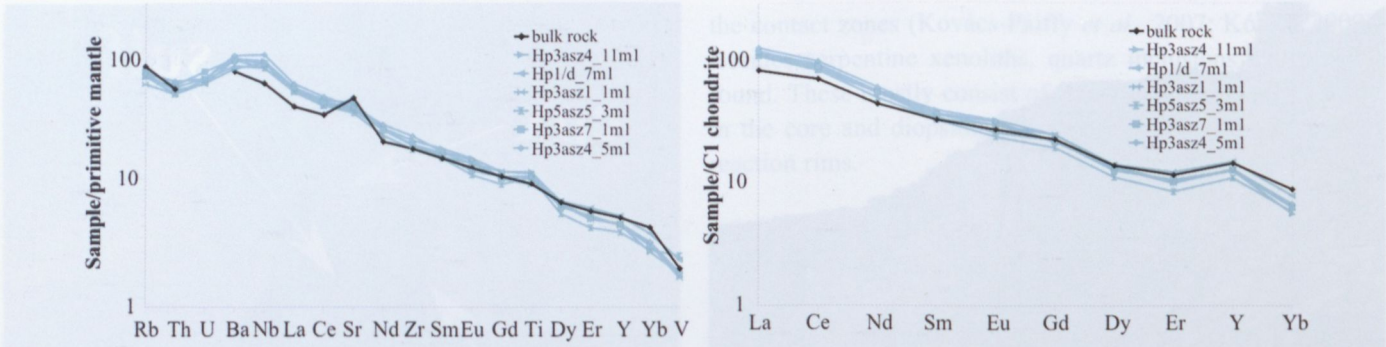

Fig. 40. Trace element composition of silicate melt inclusions (Hp3asz4_11ml, Hp1/d_7ml, Hp3asz1_1ml, Hp5asz5_3ml, Hp3asz7_1ml, Hp3asz4_5ml)) hosted in olivine phenocrysts from Haláp basalt compared to that of bulk rock of the host basalt. Multielement compositions are normalized to the primitive mantle (McDonough & Sun, 1995) and rare earth element compositions are normalized to C1 chondrite (Nakamura, 1974). Cyan coloured symbols refer to silicate melt inclusion (SMI) compositions, black symbol refers to bulk rock composition (Kóthay, 2010).

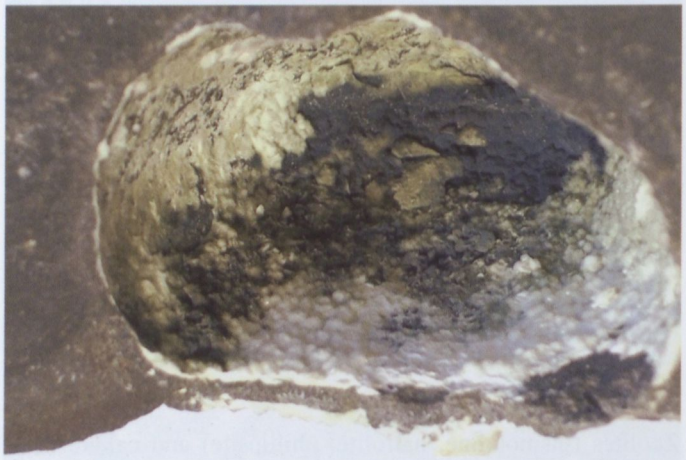

Fig. 41. White garronite with green saponite, Haláp Hill, Zalahaláp; image width: 4.5 cm.

Fig. 42. White, globular gonnardite-Na, Haláp Hill, Zalahaláp; image width: 8 cm.

colourless pseudocubic rhomboedral crystals, 3 mm in diameter. More rarely, chabazite occurs as colourless phacolite-type twins. Based on the WDS analyses, most of the crystals is *chabazite-Ca*, $(Ca_{1.75}K_{0.25}Na_{0.25}Sr_{0.01})[Al_{4.04}Si_{7.96}O_{24}]\cdot 12H_2O$. *Chabazite-Na*, $Na_{1.39}Ca_{1.04}K_{0.31}Fe_{0.01}Mg_{0.01}[Al_{4.09}Si_{7.98}O_{24}]\cdot 12H_2O$, occurs as zoned crystal with chabazite-Ca. *Garronite*, $Ca_{2.75}Na_{0.58}K_{0.16}Mg_{0.03}Ba_{0.01}Fe_{0.01}[Al_{6.11}Si_{9.83}O_{32}]\cdot 10.55H_2O$, is a very rare zeolite. It occurs as chalk-white, fibrous, spherulitic aggregates up to 1–2 mm (Fig. 41). *Gismondine*, $Ca_{0.90}Na_{0.05}K_{0.02}Mg_{0.01}[Al_{1.88}Si_{2.12}O_8]\cdot 3.78H_2O$, was found as colourless, transparent bipyramidal {232} crystals up to 2 mm. *Gmelinite* forms rare, colourless to white crystals (up to 1-2 mm) in cavities. *Gmelinite-Na*, $Na_{4.36}Ca_{1.79}K_{0.18}Ba_{0.01}Fe_{0.01}[Al_{7.78}Si_{16.12}O_{48}]\cdot 22H_2O$, was earlier identified by Szakáll *et al.* (2005). Recently a new type of gmelinite crystals have been found, which proved to be *gmelinite-Ca*, $(Ca_{2.34}Na_{1.08}K_{0.95}Sr_{0.03}Mg_{0.02}Ba_{0.01}[Al_{7.35}Si_{16.78}O_{48}]\cdot 22H_2O$. *Gobbinsite* occurs as white, lustreless globular aggregates up to 1-3 mm (Szakáll *et al.*, 2005). *Gonnardite-Na* often occurs epitaxially overgrown by prismatic natrolite. It frequently appears as white centres (up to 1.5 cm in diameter) within hemispherical natrolite aggregates (Fig. 42). The {110} prism and {111} dypiramid are dominant faces. Gonnardites have the highest Ca and lowest Na content in the lower part of the needle. Ca content decreases and Na content increases toward the top of the needle. Chemical analyses show that gonnardite shows a wide variation in CaO content (from 1.80 to 7.26). *Mesolite*, $Na_{22.53}Ca_{13.61}Fe_{0.06}Mg_{0.04}Ba_{0.04}K_{0.02}[Al_{50.11}Si_{69.90}O_{240}]\cdot 85.93H_2O$, is a rare mineral in the Haláp basalt. It rarely epitaxially intergrows with thomsonite or natrolite. *Natrolite* is a common mineral. It occurs as colourless, translucent or transparent prismatic crystals up to 4 mm in radial aggregates. The compositions of natrolite is close to the ideal formula $(Na_{1.82\text{-}1.91}Ca_{0.05\text{-}0.11}K_{0.02}Mg_{0.01}[Al_{1.96\text{-}2.05}Si_{2.94\text{-}3.03}O_{10}]$ $1.93\text{-}2.03\cdot H_2O$). Phillipsite is a very common zeolite in the Haláp quarry. It always forms complex penetration twins (Marburg and Stempel twins). Electron microprobe analyses of this mineral show that it has a very wide compositional range: phillipsite-Ca – $(Ca_{2.47}K_{0.81}Na_{0.69}Ba_{0.01}Mg_{0.01}Fe_{0.01})[Al_{6.04}Si_{9.85}O_{32}]\cdot 11.04H_2O$, phillipsite-K – $(K_{1.62}Ca_{1.25}Na_{0.87}Ba_{0.02}Mg_{0.01}Fe_{0.01})[Al_{5.49}Si_{10.62}O_{32}]\cdot 11.42H_2O$ and phillipsite-Na – $(Na_{2.46}Ca_{1.54}K_{0.33}Mg_{0.01}Fe_{0.01})[Al_{6.22}Si_{9.86}O_{32}]\cdot 12.08H_2O$ (Kónya, 2009). *Calcite* occurs as colourless to white rhombohedral crystals (up to 0.7 cm) and aggregates (up to 1.0 cm) – Generation I). Calcite always crystallized after the miarolitic

minerals. Calcite II occurs most commonly as glassy, colourless to light yellow, transparent elongated scalenohedral crystals (up to 1 cm). It precipitated after the zeolites (phillipsite + natrolite) and calcite I. *Smectite* occurs as hemispherical aggregates or forms a very thin green, brown, grey, white and rarely black coating. Smectite usually deposited on early phases (miarolitic minerals and phillipsite) but it can also be found on calcite II and natrolite-group minerals. X-ray powder diffraction data suggest that smectites are saponites. *Goethite* occurs mostly as yellow to brown coatings on earlier minerals. *Mn oxides* form brown, dendritic aggregates on zeolites and calcite (Kónya, 2009).

The miarolitic minerals crystallized first, they were followed by zeolites and calcite. Analcime and phillipsite ± chabazite/gmelinite/garronite or gobbinsite crstallised on miarolitic minerals, whereas later gonnardite-Na and natrolite crystallized from Na-rich fluids. Calcite crystallized practically continually.

3. Acknowledgements

The authors would like to express their gratitude to György Falus and Enikő Bali for their valuable contributions to the manuscript and to Tristan Azbej for technical editing and reading of the manuscript.

4. References

Bada, G. & Horváth, F. (2001): On the structure and tectonic evolution of the Pannonian basin and surrounding orogens. Acta Geologica Hungarica, **44**: 301–327.

Bali, E. (2004): Fluid/melt - wall rock interaction in the upper mantle beneath the central Pannonian Basin. PhD thesis, Eötvös University, Hungary. 160 p.

Bali, E., Szabó, Cs., Vaselli, O. & Török, K. (2002): Significance of silicate melt pockets in upper mantle xenoliths from the Bakony-Balaton Highland Volcanic Field, Western Hungary. Lithos, **61**: 79–102.

Bali, E., Falus, Gy., Szabó, Cs., Peate, D.W., Hidas, K., Török, K. & Ntaflos, T. (2007): Remnants of boninitic melts in the upper mantle beneath the central Pannonian Basin? Mineralogy and Petrology, **90**: 51–72.

Bali, E., Zajacz, Z., Kovács, I., Szabó, Cs., Halter, W., Vaselli, O., Török, K. & Bodnar, R.J. (2008a): A quartz-bearing orthopyroxene-rich websterite xenolith from the Pannonian Basin, Western Hungary: evidence for release of quartz-saturated melts from a subducted slab. Journal of Petrology, **49**: 421–439.

Bali, E., Zanetti, A., Szabó, Cs., Peate, D. & Waigh, T.E. (2008b): Evolution of the subcontinental lithospheric mantle beneath the Central Pannonian Basin: trace element evidence from silicate melt pockets in mantle xenoliths from the Bakony-Balaton Highland Volcanic Field, (western Hungary). Contributions to Mineralogy and Petrology, **155**: 165–179.

Balla, Z. (1984): The Carpathian loop and the Pannonian basin: kinematic analysis. Geophysical Transactions, **30**: 313–353.

Balogh, K. & Németh, K. (2005): Evidence for the neogene small-volume intracontinental volcanism in western Hungary: K/Ar geochronology of the Tihany Maar volcanic complex. Geologica Carpathica, **56**: 91–99.

Balogh, K. & Pécskay, Z. (2001): K/Ar and Ar/Ar geochronological studies in the Pannonian–Carpathians–Dinarides (PANCARDI) region. Acta Geologica Hungarica, **44**: 281–301.

Balogh, K., Jámbor, A., Partényi, Z., Ravaszné Baranyai, L. & Solti, G. (1982): K/Ar radigenic age of Transdanubian basalts). A Magyar Állami Földtani Intézet Évi Jelentése az 1980. évről, 243–259 (in Hungarian with English abstract).

Berkesi, M., Hidas, K., Guzmics, T., Dubessy, J., Bodnar, R.J., Szabó, Cs., Vajna, B. & Tsunogae, T. (2009): Detection of small amounts of H_2O in CO_2-rich fluid inclusions using Raman spectroscopy. Journal of Raman Spectroscopy, **40**: 1461–1463.

Bodinier, J.L., Dupuy, C. & Dostal, J. (1988): Geochemistry and petrogenesis of Eastern Pyrenean peridotites. Geochimica et Cosmochimica Acta, **52**: 2893–2907.

Bodorkós, Z. (1997): Data to the geology knowledge of the Prága Hill (Veszprém County). Folia Musei Historico-Naturalis Bakonyiensis, **16**: 49–58 (in Hungarian).

Bodorkós, Z. (2007): Historical sketch of basalt mining in the surrounding of Sümeg. Manuscript, Archive of the Museum of the Hungarian Petroleum Industry, Zalaegerszeg, Hungary (in Hungarian).

Borsy, Z., Balogh, K., Kozák, M. & Pécskay, Z. (1986): Contributions to the evolution of the Tapolca-basin, Hungary. Acta Geographica Debrecina, **23**: 79–104 (in Hungarian with English abstract).

Budai, T. & Vörös, A. (1992): Middle Triassic history of the Balaton Highland: extensional tectonics and basin evolution. Acta Geologica Hungarica, **35**: 237–250.

Cloetingh, S., Bada, G., Matenco, L., Lankreijer, A., Horváth, F. & Dinu, C. (2006): Neotectonics of the Pannonian-Carpathian system: inferences from thermo-mechanical modeling. In Gee, D.G. & Stephenson, R.A. (eds): European lithosphere dynamics. Geological Society, London, Memoirs, **32**: 207–221.

Császár, G. & Lelkesné-Felvári, G. (1999): Balaton Phyllite Formation Group. In Budai, T. & Csillag, G. (eds): Geology of the Balaton Highland. Magyar Állami Földtani Intézet, Budapest, 15–21 (in Hungarian with English abstract).

Cserny, T. (1993): Lake Balaton, Hungary. In Gierlowski-Kordesch, E. & Kelts, K. (eds): A Global Geological Record of Lake Basins, Cambridge University Press, 397–401.

Cserny, T. & Corrada, R. (1989): New results of the detailed geophysical-geological investigation of Holocen sediments and basins of Lake Balaton. A Magyar Állami Földtani Intézet Évi Jelentése az 1987. évről, 341–347.

Csillag, G., Gondárné Sőregi, K. & Koleszár, L. (1984): The key role of the basement geology in the ground-water systems in the Káli Basin. "Water resources and water conservation management of the Carpathian basin" Conference, Eger, Hungary, 136–156 (in Hungarian).

Csontos, L. (1995): Tertiary tectonic evolution of the Intra-Carpathian Area: a review. Acta Vulcanologica, **7**: 1–13.

Csontos, L. & Nagymarosy, A. (1998): The mid-Hungarian line: a zone of repeated tectonic inversions. Tectonophysics, **297**: 51–71.

Csontos, L. & Vörös, A. (2004): Mesozoic plate tectonic reconstruction of the Carpathian region. Palaeogeography Palaeoclimatology Palaeoecology, **210**: 1–56.

Csontos, L., Nagymarosy, A., Horváth, F. & Kovác, M. (1992): Tertiary evolution of the Intra-Carpathian area - a model. Tectonophysics, **208**: 221–241.

Dégi, J., Abart, R., Török, K., Rhede, D. & Petrishcheva, E. (2009): Evidence for xenolith–host basalt interaction from chemical patterns in Fe–Ti-oxides in mafic granulite xenoliths of the Bakony-Balaton Volcanic Field (W-Hungary). Mineralogy and Petrology, **95**: 219–234.

Dégi, J., Abart, R., Török, K., Bali, E., Wirth, R. & Rhede, D. (2010): Symplectite formation during decompression induced garnet breakdown in lower crustal mafic granulite xenoliths: mechanisms and rates. Contributions to Mineralogy and Petrology, **159**: 293–314.

Dobosi, G., Downes, H., Embey-Isztin, A. & Jenner, G.A. (2003a): Origin of megacrysts and pyroxenite xenoliths from the Pliocene alkali basalts of the Pannonian Basin (Hungary). Neues Jahrbuch für Mineralogie, Abhandlungen, **178**: 217–237.

Dobosi, G., Kempton, P.D., Downes, H., Embey-Isztin, A., Thirlwall, M. & Greenwood, P. (2003b): Lower crustal granulite xenoliths from the Pannonian Basin, Hungary. Part 2. Sr Nd–Pb–Hf and O isotope evi-

dence for formation of continental lower crust by tectonic emplacement of oceanic crust. Contributions to Mineralogy and Petrology, **144** (6): 671–683.

Dobosi, G., Downes, H., Mattey, D. & Embey-Isztin, A. (1998): Oxygen isotope ratios of phenocrysts from alkali basalts of the Pannonian Basin: evidence for an O-isotopically homogeneous upper mantle beneath a subduction-influenced area. Lithos, **42**: 213–223.

Downes, H. & Vaselli, O. (1995): The lithospheric mantle beneath the Carpathian Pannonian Region: a review of trace element and isotopic evidence from ultramafic xenoliths. Acta Vulcanologica, **7**: 219–229.

Downes, H., Bodinier, J.L., Thirlwall, M.F., Lorand, J.-P. & Fabries, J. (1991): REE and Sr–Nd isotopic geochemistry of eastern Pyrenean peridotite massifs: sub-continental lithospheric mantle modified by continental magmatism. Journal of Petrology, Special Lherzolites Issue, 97–115.

Downes, H., Pantó, G., Póka, T., Mattey, D.P. & Greenwood, P.B. (1995): Calc-alkaline volcanics of the Inner Carpathian arc, Northern Hungary: new geochemical and oxygen isotopic results. Acta Vulcanologica, **7**: 29–41.

Downes, H., Embey-Isztin, A. & Thirlwall, M.F. (1992): Petrology and geochemistry of spinel peridotite xenoliths from the western Pannonian Basin (Hungary) – evidence for an association between enrichment and texture in the upper mantle. Contributions to Mineralogy and Petrology, **109**: 340–354.

Drabant, A. & Mozgai, Z. (1989): Topography of mineral localities of Hungary 1. Keszthely Mountains. Ásvány- és Őslénygyűjtő Hírek, **5**: 8–11 (in Hungarian).

Embey-Isztin, A. (1976): Amphibolite/lherzolite composite xenolith from Szigliget, north of the Lake Balaton, Hungary. Earth and Planetary Science Letters, **31**: 297–304.

Embey-Isztin, A. (1984): Texture types and their relative frequencies in ultramafic and mafic xenoliths from Hungarian alkali basaltic rocks. Annales historico-naturales Musei nationalis Hungarici, **76**: 27–42.

Embey-Isztin, A. (1993): A compilation of new major, trace element and isotope geochemical analyses of the young alkali basalts from the Pannonian Basin. Fragmenta Mineralogica et Palaeontologica, **16**: 5–26.

Embey-Isztin, A. & Dobosi, G. (1995): Mantle source charasteristic for Miocene-Pleistocene alkali basalts, Carpathian-Pannonian Region: a review of trace elements and isotopic composition. Acta Vulcanologica **7**: 155–166.

Embey-Isztin, A., Scharbert, H.G., Dietrich, H. & Poultidis, H. (1989): Petrology and geochemistry of peridotite xenoliths in alkali basalts from the Transdanubian Volcanic Region, West Hungary. Journal of Petrology, **30**: 79–105.

Embey-Isztin, A., Downes, H., James, D.E., Upton, B.G., Dobosi, G., Ingram, G.A., Harmon, R.S. & Schrabert, H.G. (1993): The petrogenesis of Pliocene alkaline volcanic rocks from the Pannonian Basin, Eastern Central Europe. Journal of Petrology, **34**: 317–343.

Embey-Isztin, A., Dobosi, G., Altherr, R. & Meyer, H.P. (2001): Thermal evolution of the lithosphere beneath the western Pannonian Basin: evidence from deep-seated xenoliths. Tectonophysics, **331**: 285–306.

Embey-Isztin, A., Downes, H. & Kempton, P.D. (2003): Lower crustal granulite xenoliths from the Pannonian Basin, Hungary. Part 1: mineral chemistry, thermobarometry and petrology. Contributions to Mineralogy and Petrology, **144**: 652–670.

Erdélyi, J. (1941): Minerals of the basalt hills at Balaton. Földtani Értesítő, **6**: 60–82 (in Hungarian).

Falus, Gy. (2004): Microstructural analysis of upper mantle peridotites: their application in understanding mantle processes during the formation of the Intra-Carpathian Basin System, PhD thesis, Eötvös University, Budapest, Hungary, 163 p.

Falus, Gy. & Szabó, Cs. (2004): Upper mantle xenoliths from Tihany: traceable lithosphere evolution in the Bakony- Balaton Highland Volcanic Field. Földtani Közlöny, **134**: 499–520 (in Hungarian).

Falus, Gy., Szabó, Cs. & Vaselli, O. (2000): Mantle upwelling within the Pannonian Basin: evidence from xenolith lithology and mineral chemistry. Terra Nova, **12**: 295–302.

Falus, Gy., Szabó, Cs., Kovács, I., Zajacz, Z. & Halter, W. (2007): Symplectite in spinel lherzolite xenoliths from the Little Hungarian Plain, Western Hungary: A key for understanding the complex history of the upper mantle of the Pannonian Basin. Lithos, **94**: 230–247.

Falus, Gy., Tommasi, A., Ingrin, J. & Szabó, Cs. (2008): Deformation and seismic anisotropy of the lithospheric mantle in the southeastern Carpathians inferred from the study of mantle xenoliths. Earth and Planetary Science Letters, **272**: 50–64.

Fodor, L., Magyari, A., Kázmér, M. & Fogarasi, A. (1992): Gravity-flow dominated sedimentation on the Buda paleoslope (Hungary) - Record of late Eocene continental escape of the Bakony Unit. Geologische Rundschau, **81**: 695–716.

Fodor, L., Jelen, B., Márton, E., Skaberne, D., Car, J. & Vrabec, M. (1998): Miocene-Pliocene tectonic evolution of the Slovenian Periadriatic fault: Implications for Alpine-Carpathian extrusion models. Tectonics, **17**: 690–709.

Fodor, L., Csontos, L., Bada, G., Győrfi, I. & Benkovics, L. (1999): Tertiary tectonic evolution of the Pannonian basin system and neighbouring orogens: a new synthesis of paleostress data. In Durand, B., Jolivet, L., Horváth, F. & Séranne, M. (eds): The Mediterranean basins: Tertiary extensions within the Alpine orogen. London, Geological Society, London, Special Publication, **156**: 295–334.

Grad, M., Guterch, A., Keller, G.R., Janik, T., Hegedűs, E., Vozár, J., Slaczka, A., Tiira, T. & Yliniemi, J. (2006): Lithospheric structure beneath Trans-Carpathian transect from Precambrian platform to Pannonian basin: CELEBRATION 2000 seismic profile CEL05. Journal of Geophysical Research - Solid Earth, **111**: doi: 10.1029/2005JB003647.

Gulyás, S. (2001): The palaeogeography of Lake Balaton during deposition of the Congeria rhomboidea beds. Geologica Croatia, **54**: 2705–2712.

Haas, J., Kovács, S., Krystyn, L. & Lein, R. (1995): Significance of Late Permian Triassic facies zones and terrain reconstructions in the Alpine North Pannonian domain. Tectonophysics, **242**: 19–40.

Haas, J., Hámor, G. & Korpás, L. (1999): Geological setting and tectonic evolution of Hungary. Geologica Hungarica, Series Geologica, **24**: 179–196.

Haas, J., Mioc, P., Pamic, J., Tomljenovic, B., Árkai, P., Bérczi-Makk, A., Koroknai, B., Kovács, S. & Felgenhauer, E.R. (2000): Complex structural pattern of the Alpine-Dinaridic-Pannonian triple junction. International Journal of Earth Sciences, **89**: 377–389.

Harangi, Sz. (2001): Neogene to Quaternary volcanism of the Carpathian-Pannonian region - a review. Acta Geologica Hungarica, **44**: 223–258.

Harangi, Sz., Wilson, M. & Tonarini, S. (1995): Petrogenesis of Neogene potassic volcanic rocks in the Pannonian Basin. Acta Vulcanologica, **7**: 125–134.

Hidas, K. (2006): Petrological and geochemical characteristics of the early lithosphere beneath the Bakony-Balaton Highland Volcanic Field based on the study of xenoliths from the Tihany Volcano. MSc thesis, manuscript, Eötvös University, Budapest, Hungary. 126 p (in Hungarian with English abstract).

Hidas, K., Falus, Gy., Szabó, Cs., Szabó, P.J., Kovács, I. & Földes, T. (2007): Geodynamic implications of flattened tabular equigranular textured peridotites from the Bakony-Balaton Highland Volcanic Field (Western Hungary). Journal of Geodynamics, **43**: 484–503.

Hidas, K., Guzmics, T., Szabó, Cs., Kovács, I., Bodnar, R.J., Zajacz, Z., Nédli, Z., Vaccari, L. & Perucchi, A. (2010): Coexisting silicate melt inclusions and H_2O-bearing, CO_2-rich fluid inclusions in mantle peridotite xenoliths from the Carpathian–Pannonian region (central Hungary). Chemical Geology, **274**: 1–2, 1–18.

Horváth, F. (1993): Towards a mechanical model for the formation of the Pannonian Basin. Tectonophysics, **226**: 333–357.

Horváth, F., Bada, G., Szafián, P., Tari, G., Ádám, A. & Cloetingh, S. (2006): Formation and deformation of the Pannonian basin: constraints from observational data. Gee, D.G. & Stephenson, R.A. (eds): European lithosphere dynamics. Geological Society, London, Memoirs, 191–206.

Huismans, R.S., Podladchikov, Y.Y. & Cloetingh, S. (2001): Dynamic modeling of the transition from passive to active rifting, application to the Pannonian basin. Tectonics, **20**: 1021–1039.

Jámbor, Á. (1980): Pannonian Formations in the Transdanubian Central Range). A Magyar Állami Földtani Intézet Évkönyve, **65**: 1–259 (in Hungarian with English abstract).

Jolivet, L. & Faccenna, C. (2000): Mediterranean extension and the Africa-Eurasia collision. Tectonics, **19**: 1095–1106.

Jugovics, L. (1955): Summary geological report and calculation of reserves for the basalt occurrences Szebike and Prága Hills. Archives of the

Hungarian Office for Mining and Geology, Budapest, 129 p (in Hungarian).

Jugovics, L. (1959): Petrological study on the basalt occurrence at Mt. Haláp. A Magyar Állami Földtani Intézet Évi Jelentése az 1955–56. évről, 123–135 (in Hungarian with French and Russian abstracts).

Jugovics, L. (1971): Structure of the basalt regions of the Balaton Highland and Tapolca Basin. A Magyar Állami Földtani Intézet Évi Jelentése az 1968. évről, 223–243 (in Hungarian with German abstract).

Kázmér, M. (1990): Birth, life and death of the Pannonian Lake. Palaeogeography, Palaeoclimatology, Palaeoecology, **79**: 171–188.

Kázmér, M. & Kovács, S. (1985): Permian-Palaeogene palaeogeography along the eastern part of the Insubric-Periadriatic Linament system: evidence for continental escape of the Bakony-Drauzug Unit. Acta Geologica Hungarica, **28**: 71–84.

Kokelaar, B.P. (1983): The mechanism of Surtseyan volcanism. Journal of the Geological Society of London, **140**: 939–944.

Kónya, P. (2006): Twinned phillipsite crystals in the basalts of the Tátika Group, Balaton Highland, Hungary. 3rd Mineral Sciences in the Carpathians Conference, Miskolc, Hungary, 2006. Acta Mineralogica-Petrographica (Szeged), Abstract Series, **5**: 58.

Kónya, P. (2008): Detailed investigation of cavity-filling natrolite group minerals in basalts of Balaton Highland, Hungary. A Magyar Állami Földtani Intézet Évi Jelentése 2007-ről, 121–143 (in Hungarian with English abstract)

Kónya, P. (2009): Mineralogical and paragenetic investigations of cavity filling minerals and sedimentary xenoliths in basalts from Bakony–Balaton Highland Volcanic Field. PhD thesis, manuscript, University of Miskolc, Hungary. 303 p (in Hungarian with English abstract).

Kóthay, K. (2010): Evolution of alkali basaltic magma by use of silicate melt inclusions, based on Hegyestű and Haláp volcanoes, Bakony-Balaton Highlands. PhD thesis, manuscript, Eötvös University, Budapest, Hungary. 119 p (in Hungarian with English abstract).

Kóthay, K., Szabó, Cs., Török, K. & Sharygin, V. (2005): A droplet of the magma: silicate melt inclusions in olivine phenocrysts from alkali basalt of Hegyestű. Földtani Közlöny, **135**: 31–55 (in Hungarian with English abstract).

Kovács, I. & Szabó, Cs. (2005): Petrology and geochemistry of granulite xenoliths beneath the Nógrád-Gömör Volcanic Field, Carpathian-Pannonian Region (N-Hungary/S-Slovakia). Mineralogy and Petrology, **85**: 269–290.

Kovács, I. & Szabó, Cs. (2008): Middle Miocene volcanism in the vicinity of the Middle Hungarian zone: evidence for an inherited enriched mantle source. Journal of Geodynamics, **45**: 1–17.

Kovács, S., Szederkényi, T., Haas, J., Hámor, G. & Nagymarosy, A. (2000): Tectonostratigraphic terranes in the pre-Neogene basement of the Hungarian part of the Pannonian area. Acta Geologica Hungarica, **43**: 225–328.

Kovács, I., Bali, E., Kóthay, K. Szabó, Cs. & Nédli, Zs. (2003): Petrogenetic significance of quartz and feldspar xenocrysts in basaltic rocks. Földtani Közlöny, **133**: 397–420 (in Hungarian with English abstract).

Kovács, I., Zajacz, Z. & Szabó, Cs. (2004): Type-II xenoliths and related metasomatism from the Nógrád-Gömör Volcanic Field, Carpathian-Pannonian region (northern Hungary-southern Slovakia). Tectonophysics, **393**: 139–161.

Kovács, I., Csontos, L., Szabó, Cs., Bali, E., Falus, Gy., Benedek, K. & Zajacz, Z. (2007): Paleogene-early Miocene igneous rocks and geodynamics of the Alpine-Carpathian-Pannonian-Dinaric region: an integrated approach. In Beccaluva, L., Bianchini, G. & Wilson, M. (eds): Cenozoic Volcanism in the Mediterranean Area: Geological Society of America Special Paper, **418**: 93–112.

Kovács-Pálffy, P., Kónya, P., Földvári, M., Kákay-Szabó, O. & Bodorkós, Zs. (2007): The cavity filling minerals of the basalt from Karikás-tető (Prága Hill, Balaton Highland, Transdanubia). A Magyar Állami Földtani Intézet Évi Jelentése 2005-ről, 95–118.

Kurat, G., Embey-Isztin, A., Karcher, A. & Scharbert, H. (1991): The upper mantle beneath Kapfenstein and the Transdanubian Volcanic Region, E-Austria and W Hungary: a comparison. Mineralogy and Petrology, **44**: 21–38.

Lenkey, L. (1999): Geothermics of the Pannonian Basin and its bearing on the tectonics of basin evolution. PhD thesis, Department of Sedimentary Geology, Vrije University, Amsterdam, The Netherlands. 215 p.

Mainprice, D. (2003): "PF2k" – general purpose program for Euler angle triplets. http://www.dstu.univ-montp2.fr/TECTONOPHY/petrophysics/software/petrophysics software.html.

Majoros, Gy. (1983): Lithostratigraphy of the Permian formations of the Transdanubian Central Mountains. Acta Geologica Hungarica, **26**: 7–20.

Martin, U. & Németh, K. (2004): Mio/Pliocene phreatomagmatic volcanism in the Western Pannonian Basin. Geologica Hungarica, Series Geologica, **26**: 198.

Martin, U., Auer, A., Németh, K. & Breitkreuz, C. (2003): Mio/Pliocene phreatomagmatic volcanism in a fluviolacustrine basin in western Hungary. Journal of the Geological Institute of AS Czech Republic, **15**: 75–81.

Márton, E. (1987): Paleomagnetism and tectonics in the Mediterranean region. Journal of Geodynamics, **7**: 33–57.

Mauritz, B. (1937): Minerals formed in the vesicles of the Haláp and Gulács basalt. MTA Mathematikai és Természettudományi Értesítő, **55**: 923–937 (in Hungarian).

Mauritz, B. (1939): Minerals of the vesicles of the basalts at Haláp and Gulács Hills. Mineralogische und Petrographische Mitteilungen, **50**: 93–106 (in German).

Mauritz, B. (1948): Petrochemical study of Transdanubian basalts. Földtani Közlöny, **78**: 134–169 (in Hungarian with German abstract).

Mauritz, B. (1958): Latest mineralogical findings in Hungary. Földtani Közlöny, **88**: 447–452 (in Hungarian with German abstract).

McDonough, W.F. & Sun, S.S. (1995): The composition of the Earth. Chemical Geology **120**: 223–253.

Montagna, G., Bigi, S., Kónya, P., Szakáll, S. & Vezzalini, G (2010): Chabazite-Mg: a new natural zeolite of the chabazite series. American Mineralogist, **95**: 939–945.

Müller, P. & Magyar, I. (1992): Stratigraphical importance of Prosodacnomy-bearing Pannonian s.l. sediments from Kötcse. Földtani Közlöny, **122**: 1–38 (in Hungarian with English abstract).

Müller, P., Geary, D.H. & Magyar, I. (1999): The endemic Molluscs of the Late Miocene Lake Pannon: their origin, evolution and family-level taxonomy. Lethaia, **32**: 47–60.

Nakamura, N. (1974): Determination of REE, Ba, Fe, Mg, Na and K in carbonaceous and ordinary chondrites. Geochimica et Cosmochimica Acta, **38**: 757–775.

Németh, K., & Martin, U. (1999): Volcanism of the Tihany Volcano. In Karátson, D. (ed.) Pannon Encyclopaedia. Budapest, Hungary: Kertek 2000 Publishing House, 325–326 (in Hungarian, also available on CD ROM in Hungarian and in English).

Németh, K., Martin, U. & Harangi, Sz. (1999): Miocene maar/diatreme volcanism at the Tihany Peninsula (Pannonian Basin): The Tihany Volcano. Acta Geologica Hungarica, **42**: 349–377.

Németh, K., Korbély, B. & Karátson, D. (2000): The Szigliget maar/diatreme, Bakony- Balaton Highland Volcanic Field (Hungary). Terra Nostra (Potsdam), Proceedings for the International Maar Conference, Daun, Germany, **6**: 375–383.

Németh, K., Martin, U. & Harangi, Sz. (2001): Miocene phreatomagmatic volcanism at Tihany (Pannonian Basin, Hungary). Journal of Volcanology and Geothermal Research, **111**: 111–135.

Németh, K., White, J.D.L., Reay, A. & Martin, U. (2003): Compositional variation during monogenetic volcano growth and its implications for magma supply to continental volcanic fields. Journal of the Geological Society, **160**: 523–530.

Panaiotu, C., Pécskay, Z., Hambach, U., Seghedi, I., Panaiotu, C.E., Tetsumaru, I., Orleanu, M. & Szakács, A. (2004): Short-lived Quaternary volcanism in the Persani Mountains (Romania) revealed by combined K-Ar and paleomagnetic data. Geologica Carpathica, **55**: 333–339.

Papp, G. (2002): History of topographical and descriptive mineralogy in Hungary. Topographia Mineralogica Hungariae, **7**, 444 p (in Hungarian with a chronology and captions in English).

Patrascu, S., Panaiotu, C., Seclaman, M. & Panaiotu, C.E. (1994): Timing of rotational motion of Apuseni Mountains (Romania) – paleomagnetic data from Tertiary magmatic rocks. Tectonophysics, **233**: 163–176.

Roedder, E. (1984): Fluid inclusions. (Reviews in Mineralogy, **12**) Washington (D.C.): Mineralogical Society of America, 664 p.

Schafarzik F. (1904): Detailed description of the quarries in the territory of the Hungarian Crown. Budapest, 413 p (in Hungarian).

Seghedi, I., Downes, H., Szakács, A., Mason, P.R.D., Thirlwall, M.F., Rosu, E., Pécskay, Z., Márton, E. & Panaiotu, C. (2004a): Neogene– Quaternary magmatism and geodynamics in the Carpathian-Pannonian region: a synthesis. Lithos, **72** (3/4): 117–146.

Seghedi, I., Downes, H., Vaselli, O., Szakács, A., Balogh, K. & Pécskay, Z. (2004b): Post-collisional Tertiary–Quaternary mafic alkalic magmatism in the Carpathian-Pannonian region: a review. Tectonophysics, **393** (1–4): 43–62.

Szabó, Cs. & Taylor, L.A. (1994): Mantle petrology and geochemistry beneath the Nógrád-Gömör Volcanic Field, Carpathian-Pannonian Region. International Geology Review, **36**: 328–358.

Szabó, Cs., Harangi, Sz. & Csontos, L. (1992): Review of Neogene and Quaternary volcanism of the Carpathian–Pannonian region. Tectonophysics, **208**: 243–256.

Szabó, Cs., Harangi, Sz., Vaselli, O. & Downes, H. (1995a): Temperature and oxygen fugacity in peridotite xenoliths from the Carpathian–Pannonian Region. Acta Vulcanologica, **7**: 231–239.

Szabó, Cs., Vaselli, O., Vannucci, R., Bottazzi, P., Ottolini, L., Coradossi, N. & Kubovics, I. (1995b): Ultramafic xenoliths from the Little Hungarian Plain (Western Hungary): a petrologic and geochemical study. Acta Vulcanologica, **7**: 249–263.

Szabó, Cs., Falus, Gy., Zajacz, Z., Kovács, I. & Bali, E. (2004): Composition and evolution of lithosphere beneath the Carpathian-Pannonian Region: a review. Tectonophysics, **393**: 119–137.

Szabó, Cs., Hidas, K., Bali, E., Zajacz, Z., Kovács, I., Yang, K., Guzmics, T. & Török, K. (2009): Melt-wall rock interaction in the mantle as shown by silicate melt inclusions in peridotite xenoliths from the central Pannonian Basin (western Hungary). Island Arc, **18**: 375–400.

Szabó, Cs., Berkesi, M., Hidas, K., Guzmics, T., Bodnar, R.J. & Dubessy, J. (2010): Trace element transport by COHS fluids in the deep lithosphere: A fluid inclusion perspective. Goldschmidt Conference Abstracts 2010.

Szakáll S., Gatter I. & Szendrei G. (2005): The mineral species of Hungary. Budapest: Kőország Kiadó (in Hungarian).

Tari, G. (1991): Multiple Miocene block rotation in the Bakony Mountains, Transdanubian Central Range, Hungary. Tectonophysics, **199**: 93–108.

Tari, G., Horváth, F., Rumpler, J. (1992): Styles of extension in the Pannonian basin. Tectonophysics, **208**: 203–219.

Török, K. (2002): Ultrahigh-temperature metamorphism of a buchitised xenolith from the basaltic tuff of Szigliget (Hungary). Acta Geologica Hungarica, **45**: 175–192.

Török, K., Dégi, J., Szép, A. & Marosi, G. (2005): Reduced carbonic fluids in mafic granulite xenoliths from the Bakony-Balaton Highland Volcanic Field, W-Hungary. Chemical Geology, **223**: 93–108.

Tullner, T. & Cserny, T. (2003): New aspects of lake-level changes: Lake Balaton, Hungary. Acta Geologica Hungarica, **46**: 215–238.

Váczi, T. (2003): Mineralogical and crystallographical studies on fibrous zeolites from Hungary. MSc thesis, manuscript, Eötvös University, Budapest, Hungary (in Hungarian with English abstract).

Vaselli, O., Downes, H., Thirlwall, M., Dobosi, G., Coradossi, N., Seghedi, I., Szakacs, A. & Vannucci, R. (1995): Ultramafic xenoliths in Plio-Pleistocene alkali basalts from the Eastern Transylvanian Basin: depleted mantle enriched by vein metasomatism. Journal of Petrology, **36**: 23–53.

Vaselli, O., Downes, H., Thirlwall, M.F., Vannucci, R. & Coradossi, N. (1996): Spinel peridotite xenoliths from Kapfenstein, (Graz Basin, Eastern Austria): a geochemical and petrological study. Mineralogy and Petrology, **57**: 3–50.

Wein, G. (1969): Tectonic review of the Neogene covered areas of Hungary. Acta Geologica Hungarica, **13**: 399–436.

White, J.D.L. & Houghton, B.F. (2000): Surtseyan and related eruptions. In Sigurdsson, H., Houghton, B., McNutt, S., Rymer, H. Stix, J. (eds): Encyclopedia of volcanoes, New York: Academic Press, 495–512.

Wijbrans, J., Németh, K., Martin, U. & Balogh, K. (2007): Ar^{40}/Ar^{39} geochronology of Neogene phreatomagmatic volcanism in the western Pannonian Basin, Hungary. Journal of Volcanology and Geothermal Research, **164**: 193–204.

Wilson, M. & Downes, H. (1991): Tertiary–Quaternary extension-related alkaline magmatism in Western and Central Europe. Journal of Petrology, **32**: 811–849.

Zajacz, Z., Kovács, I., Szabó, Cs., Halter, W. & Pettke, T. (2007): Evolution of mafic alkaline melts crystallized in the uppermost lithospheric mantle: a melt inclusion study of olivine clinopyroxenite xenoliths, northern Hungary. Journal of Petrology, **48**: 853–884.

Zindler, A. & Hart, S. (1986): Chemical geodynamics. Annual Review of Earth and Planetary Sciences, **14**: 493–571.

Appendix – Itinerary for IMA2010 field trip HU5

Saturday, August 28, 2010 (Day 1)

07.00-09.00	Travel to Tihany
09.00-10.30	Field stop 1 Tihany "Szélfútta" cliffs, general geology and volcanology of Bakony–Balaton Highland, pyroclastic deposits, ultramafic xenoliths
10.30-11.30	Tihany Abbey
11.30-12.00	Travel to Monoszló, Hegyes-tű Hill
12.00-12.30	Lunch break at Hegyes-tű, Geological Exhibition
12.30-14.00	Field stop 2, Hegyes-tű, basanite
14.00-14.30	Travel to Szentbékkálla
14.00-16.00	Field stop 3, Szentbékkálla, pyroclastic deposit, granulite and ultramafic xenoliths
16.00-16.30	Travel to Badacsonytomaj
16.30-19.00	Badacsonytomaj, wine tasting and dinner
19.00-19.30	Travel to Hotel Neptun (Badacsonytomaj), accommodation

Sunday, August 29, 2010 (Day 2)

08.00-08.30	Travel to Szigliget
08.30-10.30	Field stop 4, Szigliget, "Károly" quarry, pyroclastic deposit, granulite and ultramafic xenoliths
10.30-11.30	Szigliget Castle
11.30-12.00	Travel to Bazsi
12.00-12.30	Lunch break at Bazsi, Prága Hill quarry
12.30-14.00	Field stop 5, Prága Hill quarry, alkaline basalt, minerals
14.00-14.30	Travel to Zalahaláp
14.30-15.30	Field stop 6, Zalahaláp quarry, alkaline basalt, minerals
15.30-19.00	Travel to Budapest